JGP Journal of General Physiology

VIEWPOINT

Excitation–Contraction Coupling

How does flecainide impact RyR2 channel function?

Samantha C. Salvage[1], Christopher L.-H. Huang[1,2], James A. Fraser[2], and Angela F. Dulhunty[3]

Flecainide, a cardiac class 1C blocker of the surface membrane sodium channel ($Na_V1.5$), has also been reported to reduce cardiac ryanodine receptor (RyR2)-mediated sarcoplasmic reticulum (SR) Ca^{2+} release. It has been introduced as a clinical antiarrhythmic agent for catecholaminergic polymorphic ventricular tachycardia (CPVT), a condition most commonly associated with gain-of-function RyR2 mutations. Current debate concerns both cellular mechanisms of its antiarrhythmic action and molecular mechanisms of its RyR2 actions. At the cellular level, it targets $Na_V1.5$, RyR2, Na^+/Ca^{2+} exchange (NCX), and additional proteins involved in excitation–contraction (EC) coupling and potentially contribute to the CPVT phenotype. This Viewpoint primarily addresses the various direct molecular actions of flecainide on isolated RyR2 channels in artificial lipid bilayers. Such studies demonstrate different, multifarious, flecainide binding sites on RyR2, with voltage-dependent binding in the channel pore or voltage-independent binding at distant peripheral sites. In contrast to its single $Na_V1.5$ pore binding site, flecainide may bind to at least four separate inhibitory sites on RyR2 and one activation site. None of these binding sites have been specifically located in the linear RyR2 sequence or high-resolution structure. Furthermore, it is not clear which of the inhibitory sites contribute to flecainide's reduction of spontaneous Ca^{2+} release in cellular studies. A confounding observation is that flecainide binding to voltage-dependent inhibition sites reduces cation fluxes in a direction opposite to physiological Ca^{2+} flow from SR lumen to cytosol. This may suggest that, rather than directly blocking Ca^{2+} efflux, flecainide can reduce Ca^{2+} efflux by blocking counter currents through the pore which otherwise limit SR membrane potential change during systolic Ca^{2+} efflux. In summary, the antiarrhythmic effects of flecainide in CPVT seem to involve multiple components of EC coupling and multiple actions on RyR2. Their clarification may identify novel specific drug targets and facilitate flecainide's clinical utilization in CPVT.

Introduction

Flecainide has been recognized as a class 1C antiarrhythmic agent, blocking cardiac sodium channel ($Na_V1.5$) fast currents, since preclinical studies dating back to the late 1960s (Hodess et al., 1979). It has been clinically used since 1979 to prevent or reduce ectopic ventricular events and tachycardia, atrial fibrillation (Anderson et al., 1989), and supraventricular tachycardia (Henthorn et al., 1991; Pritchett et al., 1991). It has also been beneficial in correcting long QT3 syndrome associated with gain-of-function $Na_V1.5$ mutations (Shimizu and Antzelevitch, 1999). More recently, it has been reported to also block cardiac sarcoplasmic reticulum (SR) type 2 ryanodine receptor (RyR2) ion channels (Table 1), preventing Ca^{2+} leak through the mutant RyR2 channels that underlie catecholaminergic polymorphic ventricular tachycardia (CPVT; Watanabe et al., 2009; Liu et al., 2011; Kryshtal et al., 2021).

RyR2 channels are essential for gating release of SR store Ca^{2+}, a process central to excitation–contraction (EC) coupling. The channels open in response to relatively small extracellular Ca^{2+} influxes through voltage-activated surface membrane L-type Ca^{2+} channels during cardiac EC coupling. The arrhythmias in RyR2-associated CPVT result from a sequence of events initiated by high cytosolic Ca^{2+} concentrations, $[Ca^{2+}]_i$, due to excess diastolic Ca^{2+} leak through gain-of-function mutant RyR2 channels. The resulting high end-diastolic $[Ca^{2+}]_i$ leads to delayed afterdepolarization (DAD) events, arising from increased electrogenic surface membrane Na^+/Ca^{2+} exchanger (NCX) import of 3 Na^+ for an export of 1 Ca^{2+}, acting to correct the elevated $[Ca^{2+}]_i$. Triggering proarrhythmic events can occur should the membrane potential then reach action potential threshold. There is a complex relationship between RyR2 open

[1]Department of Biochemistry, University of Cambridge, Cambridge, UK; [2]Physiological Laboratory, University of Cambridge, Cambridge, UK; [3]Eccles Institute of Neuroscience, John Curtin School of Medical Research, The Australian National University, Acton, Australia.

Correspondence to Angela F. Dulhunty: angela.dulhunty@anu.edu.au

This work is part of a special issue on excitation–contraction coupling.

Table 1. **Actions of flecainide on RyR2 channels in lipid bilayers, including RyR2 source, experimental conditions for the major experiments in each study, voltage examined and direction of current flow, and main results**

	RyR2 source	Solution ion concentrations (mM)	Voltage	Main effect of flecainide
Watanabe et al. (2009)	Sheep heart	Current carrier—Cs^+ *cis/trans* 250/250 Cs^+ *cis/trans* 2/0 ATP *cis/trans* 0.1 × 10^{-3}/1.0 Ca^{2+} *or cis/trans* 0.1/1.0 Ca^{2+}	+40 mV (current flow *cis* to *trans*)	Inhibition: IC_{50} = 15 µM: 0.1 × 10^{-3}/1.0 mM Ca^{2+} IC_{50} = 55 µM: 0.1/1.0 mM Ca^{2+}
Hilliard et al. (2010)	Sheep heart	Current carrier—Cs^+ *cis/trans* 250/250 Cs^+ *cis/trans* 2/0 ATP *cis/trans* 0.1 × 10^{-3}/1.0 Ca^{2+}	+40 mV	Open state block (+40 mV) IC_{50} = 16 µM
Hwang et al. (2011)	CSQ2$^{-/-}$ mouse heart	Current carrier—Cs^+ *cis/trans* 250/250 Cs^+ *cis/trans* 2.0/0 ATP *cis/trans* 0.1 × 10^{-3}/1.0 Ca^{2+}	+40 mV	IC_{50} for Open state block at +40 mV: Flecainide ∼16 µM R-propafenone ∼12 µM S-propafenone ∼25 µM
Mehra et al. (2014)	Sheep heart	Current carrier—Cs^+ *trans* 250 Cs^+ *cis/trans* 2.0/0 ATP *trans* 0.1 Ca^{2+} *cis* Cs^+, Ca^{2+}, Mg^{2+} concentration and pH and caffeine addition varied	+40 and −40 mV (current flow *trans* to *cis*)	Modes of block at +40 mV: (1) fast—reduced open times (2) slow—prolonged closures (3) substate with fast block (4) burst length depends on *cis* [Ca^{2+}] IC_{50} at −40 mV >100-fold greater than that at +40 mV
Bannister et al. (2015)	Recombinant human RyR2	Current carrier—K^+ *cis/trans* 610/610 KCl *cis* EMD 41000	+40 and −40 mV	1–50 µM blocks to a substate level at +40 mV No effect of 50 µM flecainide at −40 mV *trans* to *cis* flux No effect on *trans* to *cis* K^+ flux at 0 mV with 250/50 mM [K^+] No effect on *trans* to *cis* Ca^{2+} flux at 0 mV—flux driven by a 100-fold *trans* to *cis* [Ca^{2+}] gradient
Bannister et al., (2016)	Recombinant human RyR2	Current carrier—K^+ *cis/trans* 610/610 KCl *cis* EMD 41000	+40 mV and −40 mV	Flecainide analogues QX-FL and NU-FL are less potent blockers of *cis* to *trans* current *Trans* to *cis* current not altered by flecainide or its analogues
Kryshtal et al. (2021)	Sheep heart	Current carrier—Cs^+ *cis/trans* 250/250 Cs^+ *cis/trans* 2.0/0 ATP *cis/trans* 0.1 × 10^{-3}/1.0 Ca^{2+} max phosphorylation of RyR2 S2808 and S2814	+40 mV	QX-FL and NU-FL are less effective at blocking RyR2 channels but equally effective in blocking Na^+ channels, with parallel effects on SR Ca^{2+} release (Table 2)
Salvage et al. (2021a)	WT and P2328S$^{+/+}$ mouse RyR2	Current carrier—Cs^+ *cis/trans* 250/250 Cs^+ *cis/trans* 1 × 10^{-3}/1.0 Ca^{2+}	+40 mV and −40 mV	WT and mutant channels show voltage-independent (1) inhibition with ≥5 µM, and (2) activation of lower activity channels with ≥0.5 µM

Publications are listed in chronological order.

probability and the generation of Ca^{2+} sparks and waves which are major contributors to the end diastolic Ca^{2+} overload. This is discussed in more detail below.

Flecainide proved antiarrhythmic in animal CPVT models. This was suggested as a basis for its introduction in clinical CPVT therapy (Watanabe et al., 2009; Van Der Werf et al., 2011; Salvage et al., 2015, 2018). Experimental studies demonstrated that flecainide reduced excess RyR2-mediated diastolic Ca^{2+} release in CPVT models (Table 2). However, there are uncertainties bearing on the use and mechanism of action of flecainide potentially relevant to this more recent application. Indeed, despite its established history of beneficial antiarrhythmic clinical use and efficacy, flecainide also has established detrimental proarrhythmic actions in a range of other conditions. These include ischemic situations, the presence of cardiac structural changes (Echt et al., 1991; Apostolakis et al., 2013), or certain inherited cardiac conditions, particularly the Brugada Syndrome, where its therapeutic (as opposed to diagnostic) use is specifically clinically contraindicated (Salvage et al., 2018; Priori et al., 2000; Wolpert et al., 2005; Stokoe et al., 2007; Martin et al., 2010).

Uncertainties concerning flecainide action might also apply to CPVT. First, the cellular basis for its antiarrhythmic action in CPVT remains unclear and is extensively debated. Besides evidence supporting primary actions of flecainide on RyR2 channels reducing Ca^{2+} leak in some models, equally compelling evidence supports primary actions inhibiting $Na_V1.5$ channels in other CPVT models (Table 2; Watanabe et al., 2009; Liu et al., 2011; Bannister et al., 2016, 2015; Salvage et al., 2015; Kryshtal et al., 2021). Flecainide additionally has dual actions in increasing diastolic NCX activity. Its reduction of $Na_V1.5$-mediated Na^+ entry during the action potential could reduce intracellular Na^+ concentration $[Na^+]_i$ thereby favoring NCX-mediated diastolic Na^+ entry and Ca^{2+} extrusion. Flecainide can also directly activate NCX, increasing I_{NCX}, which particularly in CPVT would favor the forward-Ca^{2+} extrusion mode (Kuroda et al., 2017).

Table 2. **Effect of flecainide on RyR2 mediated diastolic Ca^{2+} release in sparks and waves, including source of cells and brief description of experimental conditions and most significant results**

Sparks, waves	Preparation	Main effect of flecainide
Watanabe et al. (2009)	ISO-stimulated intact CSQ2$^{-/-}$ myocytes	6 μM reduced the rate of spontaneous Ca^{2+} release events in the presence and absence of extracellular Na^+ and Ca^{2+}
Hilliard et al. (2010)	(1) Field stimulated intact ventricular CSQ2$^{-/-}$ myocytes. Ca^{2+} waves triggered by 100 nM ISO (2) Permeabilized rat ventricular myocytes without ISO	6 μM reduced Ca^{2+} wave rates, spark amplitude and width. Spark mass reduced by 40% Increase in spark frequency No effect on spark-mediated SR Ca^{2+} leak or SR Ca^{2+} content
Hwang et al. (2011)	(1) Field stimulated intact ventricular CSQ2$^{-/-}$ myocytes. Ca^{2+} waves with 100 nM ISO	Flecainide and R-propafenone decreased rate of Ca^{2+} waves IC_{50} of 2.2 and 1.1 μM respectively. S-propafenone much less effective. SR Ca^{2+} content not altered by any of the three drugs
Liu et al. (2011)	(1) Permeabilized mouse RyR2-R4496C$^{+/-}$ ventricular myocytes (2) Intact ventricular myocytes with ISO	Tetracaine, but not flecainide, (1) reduces spontaneous Ca^{2+} waves and sparks and (2) spontaneous Ca^{2+} release events and triggered beats, but no effect on DADs
Savio-Galimberti and Knollman (2015)	Permeabilized CSQ2$^{-/-}$ ventricular myocytes	Of all class I antiarrhythmic drugs, flecainide and R-propafenone inhibit Ca^{2+} waves with the highest potency and efficacy. Suggest reduced spark mass, not frequency, causes wave suppression.
Sikkel et al. (2013)	Intact rat ventricular myocytes with patch clamp Stimulation frequency adjusted to induce Ca^{2+} waves	5 μM did not alter Ca^{2+} transients or SR Ca^{2+} load. Ca^{2+} wave and spark frequency and wave velocity declined I_{Na} block (pharmacological or voltage-dependent inactivation) similarly reduced Ca^{2+} waves, spark frequency, and wave velocity. NCX implicated with I_{Na} change
Savio-Galimberti and Knollman (2015)	Saponin-permeabilized ventricular myocytes from CSQ2$^{-/-}$, RyR2-R4496C$^{+/-}$, C57BL/6 WT mice and WT rabbits	RyR2 activity determines the potency of open-state blockers flecainide and R-propafenone, but not tetracaine, for suppressing arrhythmogenic Ca^{2+} waves
Bannister et al. (2016)	Intact rat ventricular myocytes, drugs infused into cells through patch electrodes	Spark frequency declined with flecainide and QX-FL, but not with NU-FL No change in spark amplitude or mass with any of the compounds
Hwang et al. (2019)	CSQ2$^{-/-}$ and RyR2-R4496C$^{+/-}$ intact ventricular myocytes	Spontaneous Ca^{2+} release blocked, IC_{50} ~2 μM. Similar efficacy in both models despite different phenotype severity
Kryshtal et al. (2021)	CSQ2$^{-/-}$ ventricular myocytes	Flecainide, but not QX-FL and NU-FL, reduced Ca^{2+} wave frequency in both permeabilized myocytes (lacking surface membrane and Na^+ channels) and in voltage clamped TTX-treated myocytes

Publications are listed in chronological order. ISO, isoproterenol.

This could increase the efficiency of Ca^{2+} removal and contribute to a reduction of the excess diastolic Ca^{2+}. However, the concentration of flecainide (30 and 100 μM) demonstrated to target NCX may not be reached with therapeutic doses. Nevertheless, these features raise the possibility that flecainide alleviates clinical CPVT through combined actions on RyR2, $Na_V1.5$, and NCX.

The molecular mechanisms of RyR2 ion channel inhibition or block are also under current debate and there are many unanswered questions. A particular concern has been that, until recently, all single channel studies reported a voltage-dependent action with flecainide preventing current flow only when the ion flux was in the opposite direction to that experienced during Ca^{2+} release from the SR. This might have suggested that RyR2 was not involved in the efficacy of flecainide in treating CPVT. However, a recent study has identified a novel inhibitory effect of flecainide on isolated RyR2, that, under some experimental conditions, is independent of voltage and may contribute to the reduced Ca^{2+} release reported in cellular studies (Salvage et al., 2021a; Dulhunty et al., 2022). The same study also revealed a novel higher affinity flecainide-mediated increase of isolated RyR2 channel activity, raising the possibility that RyR2 might be involved in the proarrhythmic actions of the drug. Contrastingly, the activating effect might also contribute to the counterintuitive action of the drug in protecting against arrhythmia in loss-of-function (LOF) *RyR2* mutants associated with calcium release deficient syndrome (CRDS) seen in a murine model and in patients (Sun et al., 2021; Ormerod et al., 2021; Hirose et al., 2021). These varying anti- and proarrhythmic consequences underscore the importance of understanding the molecular mechanisms of flecainide's actions, in order to maximize its therapeutic potential, while limiting potentially fatal consequences.

How is RyR2 open probability related to Ca^{2+} leak, Ca^{2+} sparks, and Ca^{2+} waves?

Before discussing the effects of flecainide on single RyR2 channel activity, it is worthwhile considering the arrangement of RyR2 channels in vivo and the relationship between the probability of an RyR2 opening (P_o) and the generation of Ca^{2+} sparks and waves. This is a simple question with a complex answer that is still being unraveled, many aspects of which have so far been addressed only by computer modelling (Cheng and Lederer,

2008; Chen et al., 2018; Hoang-Trong et al., 2021; Iaparov et al., 2021). Simplistically, a "leak" is a small efflux of Ca^{2+} from the SR through RyR2 channels at rest or during diastole that increases cytoplasmic $[Ca^{2+}]$. This may be sufficient to activate NCX and produce the DADs that can potentially trigger arrhythmia. However, not all RyR2 channels contribute equally to such leak.

The first question is: what is the nature of the Ca^{2+} leak? It is thought to be composed of (1) Ca^{2+} released during sparks (spark leak), where Ca^{2+} is spontaneously released though clusters of 100–300 RyR2s located in calcium release units (CRUs) at dyadic junctions between the SR and transverse tubule or external surface membrane; and (2) Ca^{2+} release that is too small to generate a visible Ca^{2+} spark from clusters of 1–5 nonjunctional or rogue RyR2s (Hoang-Trong et al., 2021). This "invisible" Ca^{2+} leak can contribute 50% or more of the total diastolic leak and is therefore physiologically relevant (Santiago et al., 2010; Chen et al., 2018). The coordinated opening of RyRs during a spark is thought to be triggered by Ca^{2+} release though a single RyR2 channel in a cluster and to evolve via Ca^{2+}-induced Ca^{2+} release (CICR) with cooperative gating between neighboring RyRs (Fabiato, 1983; Cheng and Lederer, 2008; Iaparov et al., 2021). It follows that any factor (e.g., mutation) that increases the probability of an RyR2 channel opening would increase the probability of triggering a spark and therefore increase both observable and invisible leak. The characteristics of sparks can vary considerably even within one cluster depending on the connectivity of the trigger RyR to neighboring RyRs. It is greatest if the RyR2 is located centrally and least if it is at the edge (Iaparov et al., 2021; Walker et al., 2015; Chen et al., 2018). The frequency and amplitude of sparks increase when $[Ca^{2+}]_i$ increases so that neighboring CRUs can be triggered to form a compound spark (Cheng et al., 1996). The size and dimensions of a spark also depend on other parameters such as the size of the cluster and the pump–leak balance that determines whether or not SR $[Ca^{2+}]$ load is depleted by spark activity.

The second question concerns the relationship between Ca^{2+} sparks and Ca^{2+} waves. It is generally considered that Ca^{2+} waves are generated by a progressive convergence of Ca^{2+} sparks. It has been suggested that Ca^{2+} waves can be triggered by compound sparks, which then jump from one Z-disc to the next. Hoang-Trong et al. (2021) use a 3-D model of ventricular myocytes to determine calcium dynamics incorporating considerations including nonuniform release sites, stochastic calcium-leak dynamics, and nonjunctional rogue RyRs. They conclude that one CRU can trigger a neighboring cluster at distances of up to 0.6 µm away with high 99% fidelity and a delay of <8 ms. They suggest a role for small nonjunctional clusters in bridging the gap between CRUs in generating calcium waves. However, many details remain to be determined. This indeed has limited the ability of computer modelling to simulate the effects of flecainide on wave generation (Yang et al., 2016). Nevertheless, it is likely that there is a causative link between an increased probability of RyR2 channel opening under diastolic conditions, increased Ca^{2+} leak-associated spark frequency, and increased numbers of Ca^{2+} waves (Cheng and Lederer, 2008).

Voltage-dependent block of RyR2 channels by flecainide

The ability of flecainide to block RyR2 channels in a voltage-dependent manner has been extensively explored (Mehra et al., 2014; Bannister et al., 2015, 2016; Kryshtal et al., 2021). In these studies, flecainide has been shown to block the channel when the bilayer potential on the cytoplasmic side of the channel is voltage clamped to a more positive potential than that on the SR luminal side. In such a situation, cations flow from the cytoplasmic to the luminal side of the channel, in a non-physiological direction. It has also been demonstrated that flecainide does not block luminal to cytoplasmic current set by ionic gradients at 0 mV, and therefore suggested that flecainide binding on the cytoplasmic side of the pore is destabilized by current flow from the lumen, rather than the electrical potential difference across the membrane (Bannister et al., 2015); however, this hypothesis remains to be fully explored experimentally. The single channel data at face value thus does not explain the ability of flecainide to reduce diastolic Ca^{2+} leak from the SR during diastole. The physiological driving force on Ca^{2+} flux in intact myocytes is always in a direction from lumen to cytoplasm during diastole and systole because cardiac luminal SR $[Ca^{2+}]$ is always substantially higher than cytoplasmic $[Ca^{2+}]$. During diastole, luminal free $[Ca^{2+}]$ increases from a minimum of ∼300 µM to a maximum of 1–2 mM (Eisner et al., 2017). At the same time, dyadic cytoplasmic $[Ca^{2+}]_i$ decreases from an estimated maximum of ∼10 µM to a minimum of 100 nM or less (Fearnley et al., 2011). However, dyadic $[Ca^{2+}]_i$ during systole has not been measured and predicted maximum transient values can extend into the millimolar range (Peskoff and Langer, 1998; Langer and Peskoff, 1996).

Many of the single-channel experiments examining inhibitory or blocking actions of flecainide have been performed using RyR2 channels with high open probabilities (P_o > 0.8) recorded before flecainide application to maximize the blocking effects of the drug and to study the characteristics of the block (Table 1). It is unclear whether such high P_o values occur physiologically during systole, as the precise relationship between $[Ca^{2+}]_i$ and P_o cannot be measured in situ and is unknown (Bers, 2001). To achieve a high P_o with some physiological conditions, Mehra et al. (2014) used 2 mM ATP plus 100 µM Ca^{2+} in the cytoplasmic solution (with a trans $[Ca^{2+}]$ of 0.1 mM) to achieve a control P_o of 0.8–0.9 (Fig. 1, A and B). Under these conditions, two distinct mechanisms, a fast block and a slow block, were described at +40 mV. Flecainide, applied to either side of the membrane, exerted the same voltage-dependent modes of block, but with a threefold-lower potency when the drug was applied to the luminal side of the channel, indicating a requirement for cytoplasmic access to the pore. Fast block was characterized by a significant decrease in channel open time with a brief (∼1 ms) block to a substate level at ∼20% of the maximum single channel conductance, features apparent across the entire voltage range investigated, from +80 to −80 mV. Fast block occurred with a range of 100 nM to 100 µM cytoplasmic $[Ca^{2+}]$ and 100 µM to 1 mM luminal $[Ca^{2+}]$ in both the presence or absence of cytoplasmic Mg^{2+} and with a ∼0.07–0.9 range of control P_o values (Watanabe et al., 2009; Hilliard et al., 2010; Hwang et al., 2011; Mehra et al., 2014; Kryshtal et al., 2021). The voltage-dependent block of RyR2 by flecainide was correlated with an increase in Ca^{2+} spark frequency, and a reduction in Ca^{2+} spark mass and Ca^{2+} wave frequency in intact and permeabilized myocytes. All

bilayer experiments reported in these publications were performed in the presence of 2 mM cytoplasmic ATP. The P_o values reported under all these conditions fell in the high range of open probabilities recordable from the channel in bilayer situations (from 0.00001 or less to 1.00). An inherent problem with channel experiments is the difficulty in working with the very low diastolic P_o, expected with <100 nM cytoplasmic Ca^{2+} in channels from healthy animals. There are then too few open events to obtain meaningful reference measurements and it becomes even more difficult to then observe further reductions in activity with channel block.

A voltage-dependent RyR2 block to a substate level at ∼20% of the maximum conductance, similar to that described by Mehra et al. (2014), was observed only at +40 mV using a very different strategy to open the channels before applying flecainide (Table 1; Bannister et al., 2015; Bannister et al., 2016). The channels were chemically modified with 20 µM EMD 41000 (2-[2-methoxy-4-(methylthio)phenyl]-1H-imidazo [4,5-C]pyridine) dihydrochloride) to achieve a very high control P_o of 0.97–0.99 in the absence of flecainide. In initial experiments conducted in the absence of any physiological modulators such as Ca^{2+}, Mg^{2+}, or ATP in the cytoplasmic or luminal solutions, addition of ≥1 µM flecainide to the cytoplasmic side of the RyR2 channels blocked the pore only when current flow was from the cytoplasmic side to the luminal side of the channel (Fig. 1, C and D), as also shown under a variety of different conditions by Mehra et al. (2014). However, in contrast to Mehra et al. (2014), brief addition of 50 µM flecainide to the luminal side of the bilayer did not reduce RyR2 P_o, although some block of cytoplasm to luminal current was observed after 10–20 min exposure. Similar results were obtained in the same study in the absence of EMD 41000, when the channels were activated by cytoplasmic Ca^{2+} alone, with flecainide block again only apparent at +40 mV, and not at −40 mV. Finally, when the direction of current flow was set by different K^+ concentrations on either side of the bilayer at 0 mV, flecainide was effective in blocking cytoplasmic-to-luminal current, but not luminal-to-cytoplasmic current flow. Based on the cytoplasm-to-lumen current-dependence of block, these experiments would appear to suggest that the therapeutic actions of flecainide do not involve RyR2. Such a conclusion was reinforced in the same study by the lack of an effect of intracellular flecainide on Ca^{2+} spark frequency, amplitude, or mass in permeabilized ventricular myocytes, in marked contrast to earlier results (Table 2; Watanabe et al., 2009; Hilliard et al., 2010; Hwang et al., 2011).

Could flecainide reduce Ca^{2+} efflux by preventing counter current flow through RyR2?

Despite the consistent observation in bilayer experiments that flecainide is not effective in blocking current flow in a physiological direction, flecainide consistently reduced SR Ca^{2+} release and arrhythmia in mouse models of CPVT and arrhythmia in CPVT patients (Watanabe et al., 2009; Hilliard et al., 2010; Hwang et al., 2011; Mehra et al., 2014; Kryshtal et al., 2021). To rationalize these apparently contradictory observations, Bannister et al. (2021) suggested that, rather than blocking Ca^{2+} efflux, flecainide might block the counter ion current flow through RyR2 necessary to prevent a voltage developing across the SR membrane and preventing maintained Ca^{2+} efflux.

Counter current flow through RyR2

The counter current during Ca^{2+} release is essential to maintain Ca^{2+} efflux. In its absence, SR membrane potentials would reach the Ca^{2+} equilibrium potential in <1 ms, removing the electrochemical gradient driving Ca^{2+} release (Gillespie and Fill, 2008). A substantial counter current is thus necessary for a maintained large Ca^{2+} flow from SR to cytosol during physiological Ca^{2+} release events which last considerably longer than 1 ms. The ions and ion channels that might carry such a countercurrent have been the subject of investigation since the 1970s. Potential counter ions include Mg^{2+}, K^+, H^+, and Cl^-. A redistribution of Mg^{2+} into the SR was demonstrated by Somlyo (1984), and H^+ ions have also been implicated in Ca^{2+} release. However, a counter flux through known ion channels in the SR membrane, other than the RyR itself, has been discounted. Ca^{2+} release is unaffected by blocking SR K^+ channels (Fink and Veigel, 1996; Fink and Stephenson, 1987). The trimeric intracellular cation (TRIC) SR channel is not involved because caffeine-induced Ca^{2+} transients are larger than normal in TRIC knockout mice (Yazawa et al., 2007). Finally, Ca^{2+} release continues normally when Cl^- is replaced with large impermeable anions, discounting a role of SR Cl^- channels (Gillespie and Fill, 2008). A Cl^- counter current would not flow through RyR2 because the channel is impermeable to anions. A model of K^+ and Mg^{2+} counter current flow through RyR2 itself during SR Ca^{2+} release strongly supports a role for RyR2 in providing its own counter current pathway (Gillespie and Fill, 2008). If this is indeed the case, fast block of the cytoplasmic-to-luminal counter current through RyR2 by flecainide could retard Ca^{2+} release (Fig. 2; Bannister et al., 2021). Experimental proof of this hypothesis may be difficult as there is no known selective blocker of the counter current through RyR2. Also discussed is the possibility that, in addition to counter current block, RyR2 might be inhibited by flecainide binding in a voltage-independent manner to then-undiscovered sites on the RyR2 protein which could contribute to the physiological inhibition of Ca^{2+} leak through the RyR2. The existence of such sites was in fact verified experimentally and reported at much the same time (Salvage et al., 2021a).

Voltage-independent actions of flecainide

Voltage-independent RyR2 inhibition by flecainide was observed in a series of experiments on RyR2 channels from WT and homozygous RyR2-P2328S$^{+/+}$ mouse hearts (Table 1; Salvage et al., 2021a; Dulhunty et al., 2022). These experiments were performed using channels weakly activated to end-diastolic levels by a physiological [Ca^{2+}] of 1 µM on the cytoplasmic side and 1 mM on the luminal side, notably in the absence of ATP or Mg^{2+}, or other channel modulators. There was a characteristically wide range of activity in WT channels before addition of flecainide with P_o values ranging from 0.001 to 0.11 (Fig. 3, A and B). The inhibition was most clearly seen in a subset of WT channels having the highest open probabilities of 0.08 to 0.11 before exposure to flecainide in the cytoplasmic solution (Fig. 3, C and D). The channels were not affected by flecainide

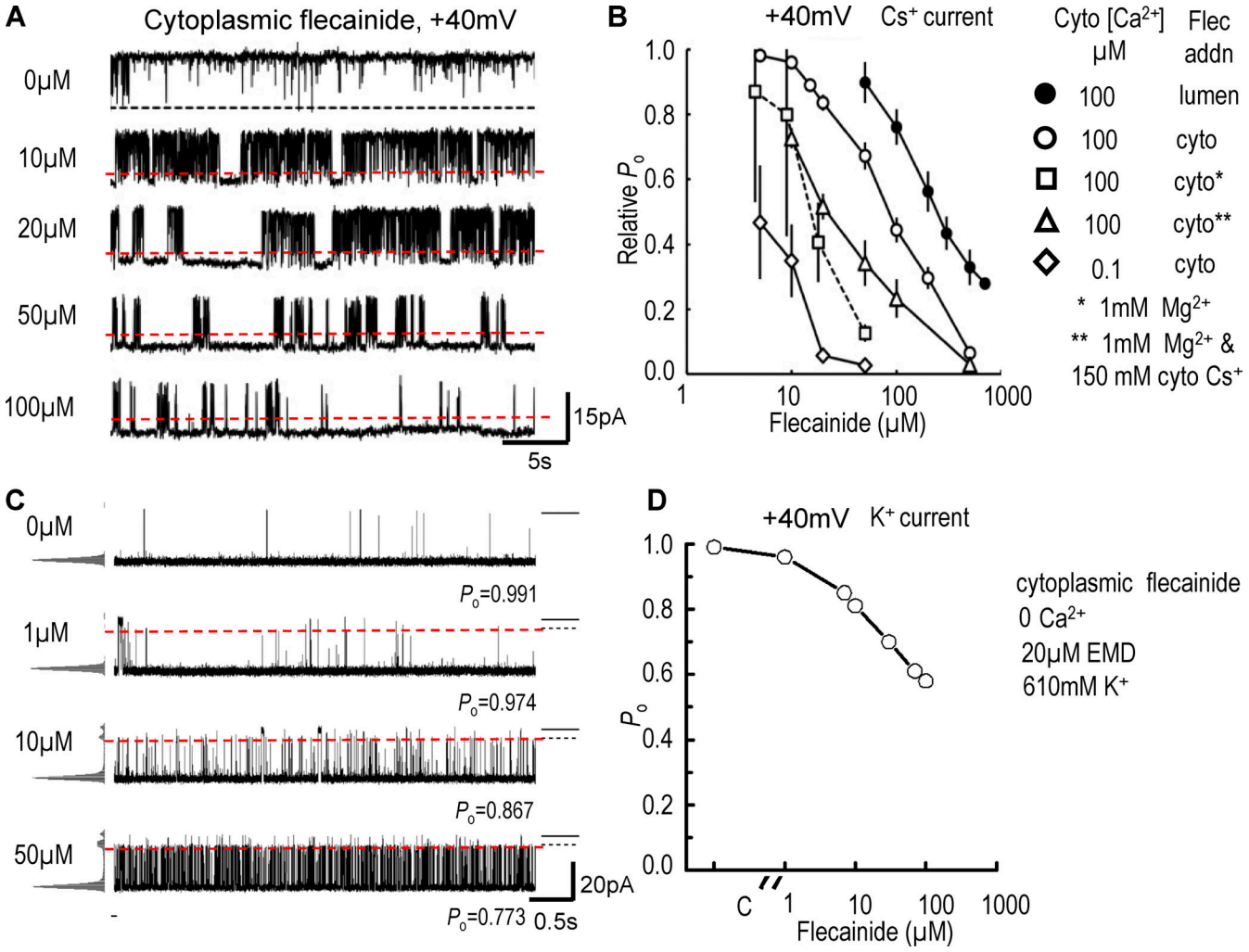

Figure 1. **Flecainide blocks RyR2 channel activity at +40 mV. (A)** Records of open channel block by flecainide (Mehra et al., 2014). Single channels from sheep RyR2 incorporated into bilayers with SR vesicles also containing triadin, junctin, and CSQ2. The bilayer potential was +40 mV (cytoplasm relative to lumen). Recordings were obtained before and after flecainide addition to the cytoplasmic bath at indicated concentrations. The cytoplasmic bath (cyto) also contained 2 mM ATP; free Ca^{2+} = 0.1 mM and free Mg^{2+} = 1 mM. The luminal bath contained 0.1 mM Ca^{2+}. Channel openings appear as upward current transitions from the baseline (channel closed level). The dashed red line indicates a possible substate level corresponding to that described by Bannister et al. (2015) and shown in C. **(B)** RyR2 open probability (P_o) expressed relative to P_o in the absence of flecainide (relative P_o) for individual channels, then average data plotted as a function of flecainide concentration. The cytoplasmic [Ca^{2+}] and the side of flecainide addition are listed with appropriate symbols beside the graph. In addition, 1 mM Mg^{2+} was added (*open squares) or 1 mM Mg^{2+} with reduced cytoplasmic [Cs^+] (**open triangles). In all conditions, the cytoplasmic solution also contained 1 mM ATP, the luminal [Ca^{2+}] was 0.1 μM, the luminal [Cs^+] was 250 mM, and the cytoplasmic [Cs^+] was 250 mM except for the open triangles where it was reduced to 150 mM. A and B were modified from Fig. 1 of Mehra et al. (2014) under copyright license # 1174586-1. **(C)** Recordings from single purified recombinant human RyR2 channels in the presence of 20 μM EMD (Bannister et al., 2015). The solutions were symmetrical, both containing 20 mM HEPES (pH = 7.4) and 610 mM KCl. In the tradition of this laboratory, channel openings at +40 mV are shown as downward transitions from the baseline, indicated by the short continuous line at the right-hand side of each recording. The flecainide-induced substate level is indicated by the short dashed line on the right side of each record and also by the superimposed dashed red line across each record in the presence of flecainide. **(D)** The effect of flecainide block on channel P_o is plotted against flecainide concentration. The graph has been modified from the original, which showed the effect of flecainide on 1-P_o, to facilitate a direct comparison with data obtained under very different conditions in B. There is a remarkable similarity to the concentration dependence of the open circle data in B. C and D were modified from Fig. 1 of Bannister et al. (2015) under copyright license #1174592-1.

concentrations <5 μM and were inhibited when flecainide was increased to concentrations of 5–50 μM. The degree of inhibition was the same at +40 and −40 mV. The decline in P_o was characterized by a strong reduction in event frequency that was mainly attributable to longer channel closures, with a weaker decrease in the duration of open events.

Voltage-independent RyR2 activation by flecainide was observed in the same series of experiments, adding to the complexity of flecainide's RyR2 actions. The activation was apparent in the majority of WT RyR2 channels, i.e., those channels having lower control open probabilities of between 0.001 and 0.08 (Fig. 3, A–C and E; Salvage et al., 2021a; Dulhunty et al., 2022). The increase in P_o was apparent with low flecainide concentrations of 500 nM and 1 μM and was clearly seen at positive and negative potentials (Fig. 3, A and B). Voltage-independent inhibition was also apparent in a biphasic effect

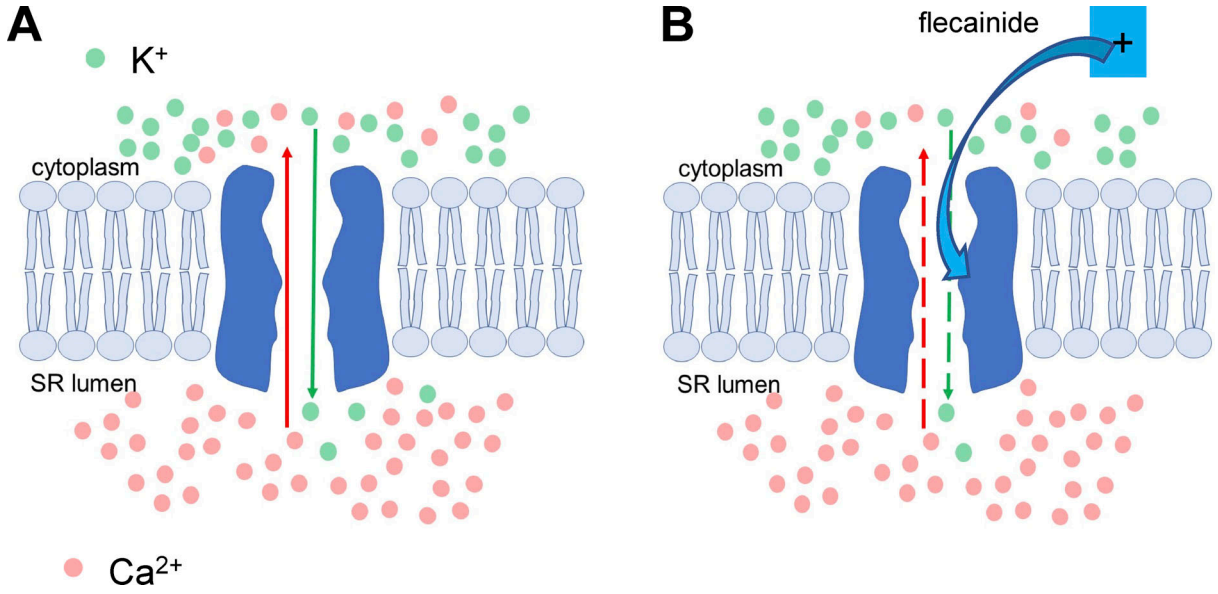

Figure 2. **A cartoon illustrating the hypothetical action of flecainide in occupying/binding in the RyR2 pore. (A)** In the absence of flecainide Ca^{2+} flow from the SR to the cytoplasm is facilitated by a largely K^+-mediated counter current from the cytoplasm into the lumen. **(B)** The positively charged flecainide when added to the cytoplasmic solution moves into the pore where it is too large to pass through the selectivity filter and remains trapped (Bannister et al., 2021). In this situation, flecainide partially blocks the K^+ counter current flowing into the SR during Ca^{2+} release and thus reduces Ca^{2+} flow through the channel. Bannister et al. (2021) suggest that retarding the charge compensation via partial/substate block of a cytoplasmic-to-luminal counter-current through RyR2 may result in inhibition of Ca^{2+} release.

of flecainide in these low activity channels with the degree of activation declining at higher flecainide concentrations, likely due to the onset of the inhibitory effect (Fig. 3 E). The increased P_o was attributable to an increase in event frequency, with inconsistent changes in open and closed times, possibly due to the overlapping influences of activation and inhibition. This was the first report of RyR2 activation by flecainide, although there have been previous indications of a high-affinity activation. For example, Fig. 5 A of Hilliard et al. (2010) shows records from one channel in which P_o is greater than control with 20 µM flecainide and then decreases with 50 µM flecainide. Overall, most of the available literature indicates that the cellular effect of flecainide on RyR2 is a reduction of SR Ca^{2+} efflux reflected in its clinical antiarrhythmic effectiveness in CPVT. Under these in vivo conditions the channel activity is influenced by the full complement of regulatory factors, including associated proteins such as triadin, junctin, calsequestrin, and calmodulin. However, the existence of an additional voltage-independent activation site raises the possibility that the drug might increase RyR2 activity under adverse conditions such as acquired heart disease, where flecainide is proarrhythmic and is contraindicated. Flecainide activation might also be exposed in the presence of other factors such as drugs or RyR2 mutations. Indeed, RyR2 activation by flecainide may well contribute to an unexplained increase in spark frequency observed in myocytes at the same time as the decrease in spark mass (Hilliard et al., 2010).

A voltage-independent substate stabilized by flecainide

RyR opening to substate levels (subconductance levels) is a common property of recombinant RyR channels and those isolated from muscle, under a wide variety of conditions (Liu et al., 1989; Ahern et al., 1997; Bhat et al., 1999; Salvage et al., 2019). Subconductance openings in mouse RyR2 channel activity at +40 and −40 mV are seen before exposure to flecainide and are more apparent in many WT and P2328S channels following exposure to flecainide (Figs. 3, 4, and 6; Salvage et al., 2021a; Dulhunty et al., 2022). This substate activity is therefore intrinsic and enhanced by flecainide, in contrast to the substate that is induced by flecainide and is described in more detail below. Also discussed below is the likelihood that the enhanced intrinsic substate activity contributed to the activation of RyR2 by low concentrations of flecainide.

Multiple actions of flecainide on single RyR2 channels—how many flecainide binding or interaction sites?

The literature cited in the previous sections indicates multiple actions of flecainide and suggests that there are multiple flecainide binding sites in the RyR2 protein (Table 3 and Fig. 5). The existence of multiple binding sites may not be surprising given that the drug shows a relatively high degree of promiscuity. In addition to its inhibition of RyR2 and its classical IC inhibitory actions on peak I_{Na} ($Na_V1.5$), flecainide inhibits the skeletal muscle I_{Na} ($Na_V1.4$; Desaphy et al., 2004) and a number of potassium channels including $K_V1.5$ (I_{Kur}), $K_V4.2$ (I_{Tof}), and $K_V11.1$/hERG (I_{Kr}) as detailed in Salvage et al. (2018), as well as directly activating NCX1 (Kuroda et al., 2017). As such it is not surprising that there may be several binding sites on RyR2, which is the largest of the known ion channels with a vast exposed cytoplasmic surface, which could convey multiple contrasting inhibitory and activating effects (Mehra et al., 2014; Salvage et al., 2021a; Dulhunty et al., 2022). This section, along

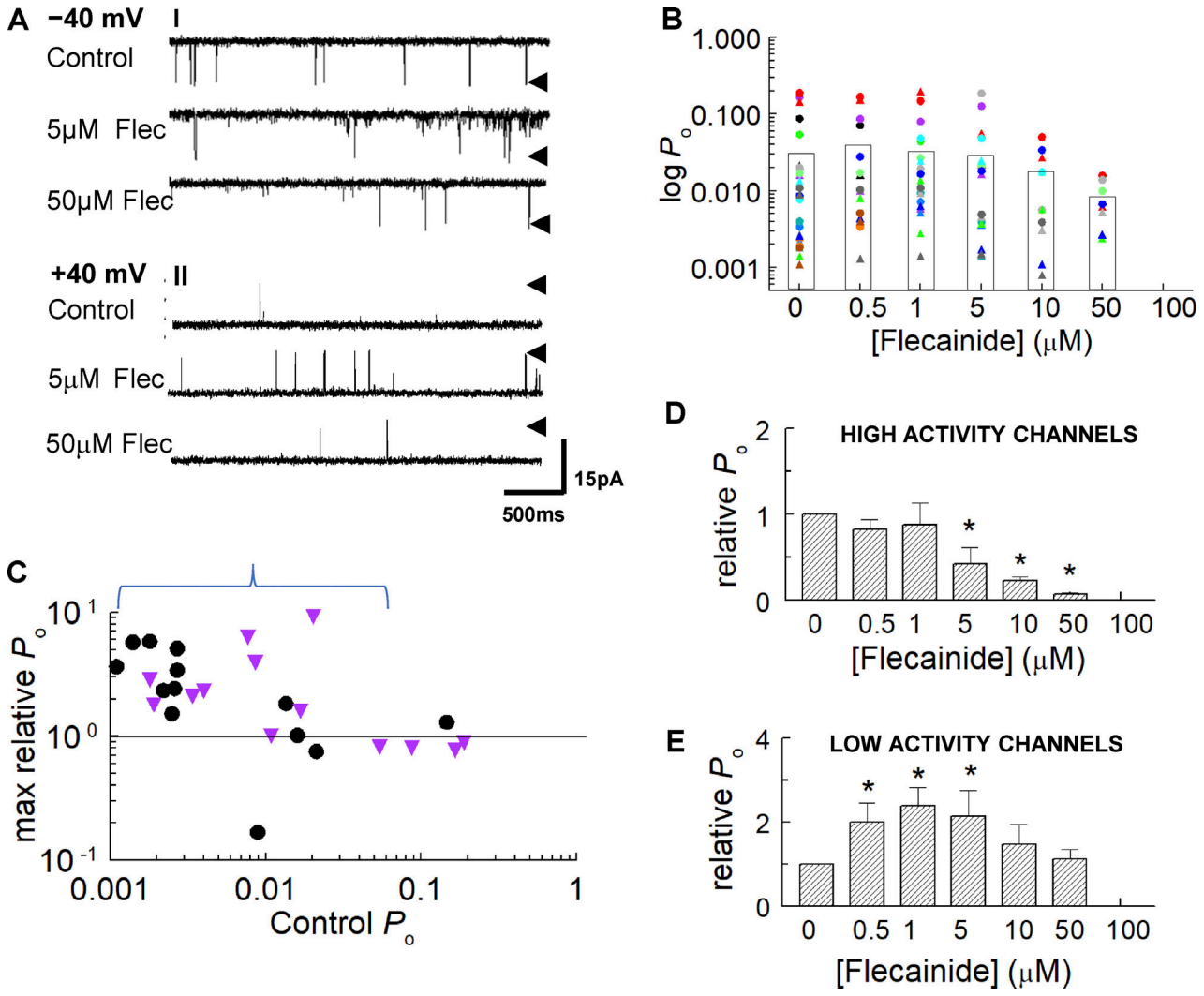

Figure 3. **Flecainide can exert a voltage-independent inhibitory action on high activity RyR2 channels.** Data is shown for mouse RyR2 channels isolated from WT littermates of homozygous RyR2-P2328S$^{+/+}$ mice (Salvage et al., 2021a). **(A)** Representative channel currents before addition of flecainide (upper) and with 5 μM flecainide (middle) and 50 μM flecainide (lower) at −40 mV, with channel opening downward (A, I) and +40 mV, with channel opening upward (A, II). Arrows indicate maximum open current level. **(B)**. Individual relative P_o data at +40 mV (circles) and −40 mV (triangles). Data for each channel is represented by symbols of the same color. The data in this graph illustrates the voltage-independence of changes with flecainide and suggests a decline in activity as flecainide concentration increases in channels with high control P_o values, in contrast to an increase in activity in channels with a lower control P_o. The boxes indicate the average P_o for each flecainide concentration. **(C)** Individual maximum relative P_o values with flecainide, plotted against control P_o. Black circles, +40 mV; purple triangles, −40 mV. Maximum relative P_o is the highest value recorded over 60–90 s segments of activity with flecainide in each channel across all concentrations of the drug. Values below 1 indicate that there was no increase in activity at any concentration, but do not reflect the full decline in activity. The full decline in activity for individual channels is shown in B. The graph in C shows that all channels with an initial activity <0.02 demonstrated substantial periods of activation during exposure to flecainide, while channels with initial activity >0.08 did not show similar periods of increased activity. **(C–E)** The upper opening bracket indicates channels included in the low control activity group (E). The remaining channels are included in the high activity group in D. D and E show average relative P_o values for high (D) and low (E) activity channels at individual flecainide concentrations. The high activity channels show a significant decline in activity with 5–50 μM flecainide. The low activity channels show significant increases in activity with 0.5–5 μM flecainide. Single-channel traces and graphs are from Salvage et al. (2021a).

with Table 3 and Fig. 5, summarises the various actions of flecainide and the potential binding sites.

Fast voltage-dependent block of RyR2 by flecainide

Fast open channel block, whether of Ca^{2+} efflux or counter current, is independent of P_o before drug application and is characterized by brief 1 ms channel closures (Mehra et al., 2014). Fast block is most sensitive to cytoplasmic application of the drug and to cytoplasmic pH. This suggests binding to a site accessible from the cytoplasmic side, located near the transmembrane domain and influenced by the electric field across the membrane. The effect of the electric field on flecainide is analogous to the response of voltage sensors, which sense electric field by movement of charges or dipoles within the membrane (Bezanilla, 2008) and also analogous to movement of H^+ ions through Na^+ channels (Woodhull, 1973). The voltage-dependent block of RyR2 depends on the ionic charge of flecainide as well as the relative positions of the flecainide binding sites in the

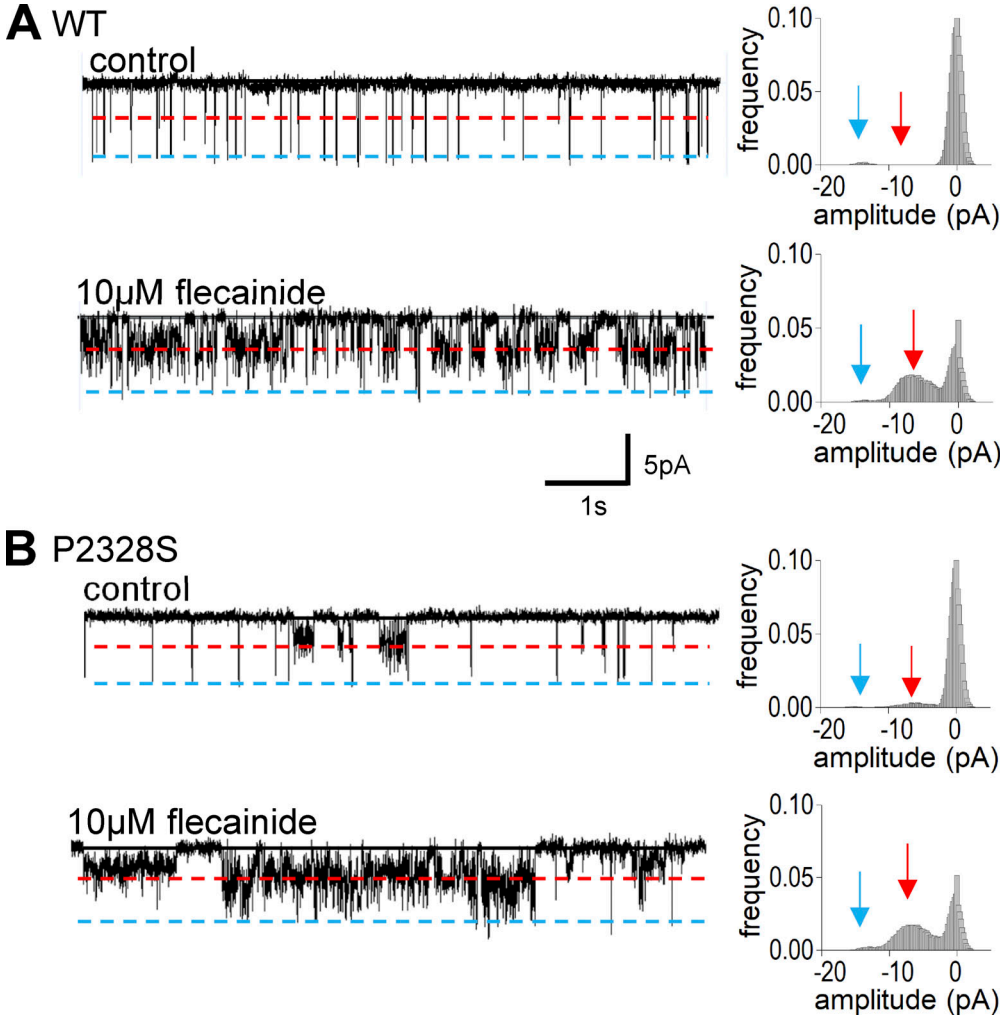

Figure 4. **Substate activity is stabilized by flecainide in RyR2 channels from WT and homozygous RyR2-P2328S$^{+/+}$ mouse hearts.** Examples of flecainide-stabilized substate activity seen in channels analyzed for datasets shown in Figs. 3 and 6. **(A and B)** Data for WT channels (A) and data for the P2328S channels (B). In A and B, examples of single channel recordings at −40 mV are shown with channel opening downward. The all-points frequency histograms for each channel are shown on the left. The upper record in each panel shows control activity and the lower recording shows activity from the same channel after exposure to 10 μM flecainide. The red lines in the records and red arrows in the histograms indicate the main substate level. The blue lines and blue arrows indicate the maximum channel conductance levels. The black lines in the records show the zero current closed level.

membrane field (Mehra et al., 2014). The binding site is likely to be within the channel pore, in a similar location to that shown convincingly with flecainide block of the $Na_V1.5$ and $K_V11.1$/hERG channels. Although both the on- and off-rates of fast RyR2 block by flecainide are voltage-dependent, this voltage dependence was not consistent with the Woodhull model. An alternative model in which voltage-dependence is due to distortion of the binding site by the electric field (Chopra et al., 2009) provided a better fit to the data.

Slow voltage-dependent channel block by flecainide

As with fast block, slow block is most sensitive to cytoplasmic application of flecainide and to cytoplasmic pH, indicating that the binding site is located on the cytoplasmic side of the pore (Mehra et al., 2014). However, other characteristics of slow block differ from those of fast block, suggesting a different binding site. In contrast to fast block, slow block is characterized by long closures lasting ~1,000 ms and is most apparent in RyR2 channels that have a relatively low open probability before flecainide application. In addition, the on-rate of slow block is voltage-dependent, but the off-rate is independent of bilayer potential. The Woodhull model predicted that the binding site for the slow block was closer to the luminal bath potential than the cytoplasmic potential. These model-dependent differences between the two modes of block also suggest different interaction sites for flecainide within the channel pore.

The flecainide-induced substate

The flecainide-associated substate level was identified in sheep RyR2 and in recombinant human RyR2 and was observed only after the addition of flecainide (Mehra et al., 2014; Bannister et al., 2015). Although its conductance was measured at all potentials from +80 to −80 mV, its characteristics at negative potentials have not been addressed (Mehra et al., 2014). Bannister

Table 3. **Potential flecainide binding or interaction sites on RyR2 that have been implicated in single channel lipid bilayer studies**

Binding site#	Mechanism	Voltage dependence	Likely location	Effective [flecainide] range given or IC_{50}/AC_{50}	Significant characteristics	
#1a[a]	Open state fast block P_o↓, T_o↓, T_c↕	+40 mV only	Cytoplasmic in the transmembrane domain	IC_{50} 15–17 µM	IC_{50} with diastolic $[Ca^{2+}]$s independent of P_o	Watanabe et al. (2009) Mehra et al. (2014) Bannister et al. (2015)
#1b[1]	Flecainide-induced substate	Described at +40 mV only	Cytoplasmic in the transmembrane domain	40–500 µM (Mehra) or 1–50 µM (Bannister)	Appears to be mainly associated with fast block	Mehra et al. (2014) Bannister et al. (2015)
#2[a]	Slow block T_c↑	+40 mV only	Cytoplasmic in the transmembrane domain	50–100 µM	Most apparent in low P_o channels	Mehra et al. (2014)
#3[1]	Burst inhibition P_o↓, T_o↓, T_c↕	+40 mV only	Cytoplasmic in the transmembrane domain	20–50 µM	*cis* 2 mM ATP and 0.1 µM Ca^{2+}	Hilliard et al. (2010) Mehra et al. (2014)
#4a	Activation P_o↑, T_o↕, T_c↕, F_o↑	+40 and −40 mV	Cytoplasmic peripheral	0.5–5.0 µM	Mainly in low activity RyR2 P_o < 0.08	Salvage et al. (2021a)
#4b[1]	Flecainide-stabilized substate P_o↑, T_o↑, T_c↓	+40 and −40 mV	Cytoplasmic peripheral	5.0–10 µM	Mainly in low activity RyR2 P_o < 0.08	Salvage et al. (2021a) Figs. 3, 5, and 6 in this manuscript
#5	Inhibition P_o↓, T_o↕, T_c↑, F_o↓	+40 and −40 mV	Cytoplasmic peripheral	10–100 µM	Mainly in high activity RyR2 P_o > 0.08	Salvage et al. (2021a)

Changes in channel gating parameters (P_o, T_o, T_c, F_o) are given relative to control values before flecainide addition, where data is given in publications or inferred from publication figures. Increase indicated by ↑, decrease indicated by ↓, and no significant effect indicated by ↕. #1b[1], The flecainide-induced substate appears to be a component of fast block and is suggested to be a function of number of flecainide molecules in the pore (Mehra et al., 2014), although the possibility that it is the result of flecainide binding to an additional binding site has not been excluded. #3[1], The effect of flecainide in reducing burst activity may be an independent mechanism and separate binding site in the pore (Mehra et al., 2014), or could be explained by a component of transitions between fast and slow block with 100 nM cytoplasmic Ca^{2+}. #4b[1], The flecainide-stabilized substate is tentatively attributed to the activation site. The substate must contribute to activation, but the relative contributions from maximal and substate openings have not been dissected. It remains possible that the stabilization is the result of flecainide binding to separate substate sensitive sites.
[a]Fast and slow block are apparent in the same records. Slow block clearly increases the closed times, but T_o for slow block was not separated from the reduction in T_o as a result of fast block.

et al. (2015) also describe the substate in conjunction with channel block. This substate appears to dominate activity even when openings to the maximum conductance were strongly inhibited at −60 mV by 500 µM flecainide (Fig. 7 of Mehra et al., 2014). It is unclear whether the flecainide-induced substate a part of the same process as fast block or slow block or the result of a separate binding reaction. In the following discussion, we have included the flecainide-induced substate with the fast block mechanism (Table 3 and Fig. 5).

Burst activity abbreviation by flecainide

A fourth voltage-dependent inhibitory mechanism inducing burst activity is induced by flecainide (Hilliard et al., 2010; Mehra et al., 2014). Long openings were observed during control activity of RyR2 channels exposed to an end-diastolic cytoplasmic $[Ca^{2+}]$ of 100 nM. During the fast block by flecainide, the long openings were replaced by recurrent bursts of activity separated by relatively long closures. The duration of the bursts became shorter with increasing flecainide concentration, with an IC_{50} of 15 µM. The burst activity is suggested to be another fast mechanism of inhibition by flecainide that may depend on flecainide binding to, or interacting with, a separate site on RyR2 (Mehra et al., 2014).

Voltage-independent RyR2 inhibition by flecainide

The voltage-independent mechanism suggests that flecainide can bind to an inhibitory site located outside the membrane field, presumably on the cytoplasmic side of the protein and therefore distinct from the three modes of voltage-dependent block (Fig. 5; Salvage et al., 2021a). It is likely that this site is on the large regulatory cytoplasmic domain of the protein which contains binding sites for many of the regulatory ligands associated with the RyR2 (Meissner, 2017).

Voltage-independent RyR2 activation by flecainide

The increase in activity when RyR2 channels with relatively low activity are exposed to low concentrations of flecainide was attributed to flecainide binding to a higher affinity activation site, which was remote from the influence of the membrane electric field. As with the voltage-independent inhibitory site, the novel activation site is most likely located on the large cytoplasmic domain of the protein (Fig. 5; Salvage et al., 2021a).

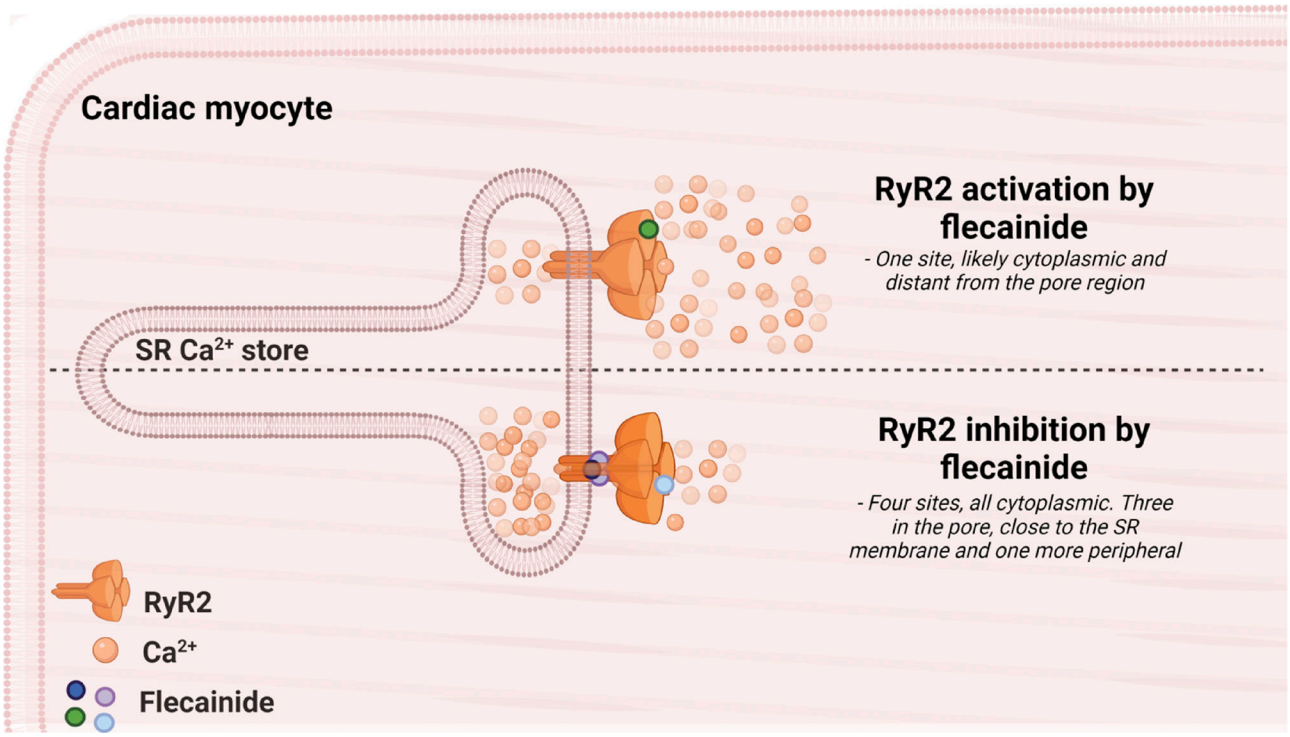

Figure 5. **A model showing multiple binding sites for flecainide in the RyR2 channel protein.** The RyR2 channels, consisting of four subunits, are shown embedded in the SR membrane. The channel in the upper half of the figure is shown with flecainide bound to a peripheral activation site on one of the subunits. The channel in the lower half of the figure is shown with flecainide bound to four inhibitory sites. One inhibitory site is located on the periphery, distant from the pore. The peripheral locations are suggested by the voltage-independence of the effects of binding to these sites. The other three inhibitory sites support voltage-dependent functions and are thus located close to the membrane; one is within the pore partially blocking ion transport as shown in Fig. 2. The other two voltage-dependent inhibitory sites are associated with the transmembrane domain and directly influence channel gating. The model is modified from the graphical abstract for Salvage et al. (2021a), and was created with biorender.com, agreement no. WT23G9D9FH.

The voltage-independent substate stabilized by flecainide

The stabilization of intrinsic substate activity is another voltage-independent action of flecainide and contrasts with the voltage-dependent fast block–associated substate which is induced by flecainide (see The flecainide-induced substate). The question is whether this substate stabilization represents yet another binding site for flecainide. This question will remain difficult to answer until the molecular mechanisms that underly the multiplicity of substates present, particularly in mouse RyR2 activity under a variety of conditions (Salvage et al., 2019), have been determined. As discussed below, current passing through the flecainide-stabilized substate contributes to the increase in P_o seen with low concentrations of flecainide. Therefore, the actions of flecainide in stabilizing substate activity and in activating the channel are tentatively attributed to one site in the discussion of potential binding sites (Table 3 and Fig. 5). However, it remains possible that the stabilization is the result of flecainide binding to separate substate-sensitive sites.

At least five potential flecainide binding sites

In summary, with the evidence presented above, we suggest that there are at least five potential binding sites on the RyR2 protein for flecainide (Table 3 and Fig. 5). Strongly supported are the voltage-dependent fast open channel block and slow block and the effect on bursting activity (Mehra et al., 2014), as well as the voltage-independent inactivation and activation including intrinsic substate stabilization (Salvage et al., 2021a). Less certain is whether additional binding sites are required for the flecainide-induced substate and the flecainide-stabilized substate. The voltage-independent binding sites are assumed to be on the extensive cytoplasmic domain of the protein, rather than the luminal domain: high-resolution cryo-EM demonstrates that the luminal domain is tiny (Peng et al., 2016). Furthermore, the luminal domain is likely to have restricted drug accessibility due to the number of regulatory proteins such as triadin, junction, and CSQ2, known to remain associated with the small luminal domain of RyR2 channels in SR vesicles incorporated into bilayers (Groh et al., 1999; Beard et al., 2002; Beard et al., 2004; Györke et al., 2004; Li et al., 2015). Nevertheless, the location of the voltage-independent binding sites requires further investigation.

Which residues form the voltage-dependent flecainide binding sites in the RyR2 pore?

The specific locations of the voltage-dependent flecainide binding sites are similarly unknown. The binding sites may have characteristics in common with the voltage-sensitive flecainide binding sites in sarcolemmal ion channels. To block both $Na_V1.5$ and $K_V11.1$/hERG channels, flecainide accesses its binding site on the inner cavity of the central pore from the cytoplasmic side in

a use-dependent manner with channel gating (Ragsdale et al., 1994; Melgari et al., 2015; Salvage et al., 2018). The binding site in $Na_V1.5$ is likely to be phenylalanine 1759 in the IV-S6 helix that forms part of the channel pore. The high-affinity binding of the local anaesthetic lidocaine to $Na_V1.5$ depends on cationic interactions with this residue (Ahern et al., 2008) and the positively charged flecainide could interact with the same site in $Na_V1.5$. In silico analysis suggests that once flecainide is docked to this site, it occupies a hydrophobic cavity at the interface of adjacent subunits and makes contact with phenylalanine 1759 in IV-S6 (Salvage et al., 2018). Similar binding sites in the channel pore are suggested for K^+ channel block by flecainide (Melgari et al., 2015). In addition, flecainide is effective in treating myotonia in skeletal muscle by blocking the skeletal $Na_V1.4$ channel, again through accessing pore sites from the cytoplasm. There are differences between the effects of flecainide on $Na_V1.4$ and $Na_V1.5$ channels consistent with structural differences between these cardiac and skeletal channels (Desaphy et al., 2004). We have not found any reports of flecainide or local anesthetic binding to these ion channels at sites outside the transmembrane pore. However, the mode of flecainide binding to NCX1 (Kuroda et al., 2017) has yet to be established, but will presumably differ from binding to the pore helices in Na^+ and K^+ channels.

Correlations between channel observations and flecainide's therapeutic actions in vivo

Flecainide interactions with RyR2 reducing Ca^{2+} waves in myocytes

Within the cell, the efficacy of flecainide in reducing RyR2 activity is likely to depend on pH as well as the cytoplasmic concentrations of ATP, Mg^{2+}, and Ca^{2+} (Mehra et al., 2014), with diastolic $[Ca^{2+}]_i$ being consistently perturbed in CPVT (Priori et al., 2001; Knollmann et al., 2006). In addition, RyR2 does not exist alone in myocytes. It occurs in a complex with interacting regulatory proteins including FKBP12/12.6, triadin, junctin, CSQ2, and calmodulin, which all have specific influences on RyR2 function (Dulhunty et al., 2012) and may influence flecainide binding to RyR2 and consequent effects on channel activity, with variations between health and disease. The single RyR2 channels examined by Watanabe et al. (2009) and subsequent manuscripts from that laboratory, as well as those in Salvage et al. (2021a) and Salvage et al. (2019) were embedded in native SR vesicles and therefore remained associated with FKBP12/12.6, triadin, junctin, and CSQ2 (Wei et al., 2009; Beard et al., 2002). It is notable that the flecainide block observed in recombinant purified human RyR2 channels examined by Bannister et al. (2015) and Bannister et al. (2016) was similar to the fast block observed in native sheep RyR2 (Watanabe et al., 2009; Mehra et al., 2014). Despite the voltage-dependence of this block which suggests that it could not contribute physiologically, there is no doubt that flecainide has proved an effective treatment for CPVT in the absence of structural disease. Other more specific $Na_V1.5$ channel blockers such as lidocaine and procainimide are less effective in treating RyR2-dependent CPVT, indicating that RyR2 is an important target in flecainide's CPVT efficacy (Watanabe et al., 2009; Van Der Werf et al., 2011; Steele et al., 2013; Salvage et al., 2018; Bannister et al., 2021). Unresolved questions are whether a fast voltage-dependent block of the counter current through the RyR2 pore could contribute to this efficacy and whether voltage-independent inhibition of Ca^{2+} efflux (Salvage et al., 2021a; Dulhunty et al., 2022) also plays a role in reducing Ca^{2+} leak in intact cells.

Flecainide efficacy in CPVT depends on interactions with RyR2 and other EC coupling proteins

As mentioned previously, flecainide is promiscuous and interacts directly with several critical cardiac EC coupling proteins. The cascade of events leading to systolic SR Ca^{2+} release is initiated by surface membrane action potentials generated by I_{Na} through $Na_V1.5$ channels producing an influx of extracellular Na^+. The Na^+ channel-mediated depolarization then opens $Ca_V1.2$ channels allowing the small extracellular Ca^{2+} influx that activates RyR2 channels through CICR. The resulting massive cytoplasmic $[Ca^{2+}]$ increase causes contraction. The system is reset by SR Ca^{2+} reuptake via SR, ER Ca^{2+} ATPase (SERCA) activity and by Ca^{2+} extrusion by surface NCX. CPVT arrhythmia is generated by excess Ca^{2+} release through mutant RyRs during diastole and this higher than normal cytoplasmic $[Ca^{2+}]$ impacts on the activity of RyR2 itself, $Na_V1.5$ channels and on NCX. Flecainide can bind to and dramatically alter the function of $Na_V1.5$, RyR2 (as discussed above) and NCX (Kuroda et al., 2017). Flecainide binding activates NCX, in contrast to its inhibitory action on $Na_V1.5$. The situation is complicated by the fact that the functions of the three proteins are interdependent. All three proteins are important in setting $[Ca^{2+}]_i$ as well as being directly influenced by $[Ca^{2+}]$. There is considerable debate about whether flecainide blocking $Na_V1.5$, blocking RyR2 or activating NCX is most important in the overall efficacy of flecainide and the specific experimental protocols designed to explore the question can influence the outcome of the experiments (Steele et al., 2013). The arguments will not be considered here as they have been addressed in detail elsewhere (Salvage et al., 2018; Steele et al., 2013; Sikkel et al., 2013; Kryshtal et al., 2021; Priori et al., 2021). It is most likely that the antiarrhythmic efficacy of flecainide in CPVT results from its actions in appropriately modifying the activity of all three of these proteins that are integral to restoring effective EC coupling and whose functions are disrupted by excess Ca^{2+} release through RyR2 (Steele et al., 2013; Sikkel et al., 2013; Salvage et al., 2018).

Contribution of NCX to CPVT and flecainide efficacy

At this point, it is worth briefly considering the overall complex contribution of NCX to changes in $[Ca^{2+}]_i$ during systole/diastole of the cardiac cycle and to likely changes with CPVT and to the actions of flecainide in intact myocytes. NCX is an electrogenic bidirectional transporter providing one of the major pathways by which cytosolic Ca^{2+} levels are tightly regulated (Bers, 2000; Blaustein and Lederer, 1999). For most of the cardiac cycle, the electrochemical driving force, determined by the membrane potential and concentration gradients of both Na^+ and Ca^{2+} across the sarcolemma, favors forward mode Ca^{2+} extrusion. This generates a small inward current (I_{NCX}) due to the entry of 3 Na^+ for every 1 Ca^{2+} exported. Reversal of NCX to support Ca^{2+}

entry during the action potential depends on the membrane potential exceeding −40 mV and an increase of cytosolic Na^+ (Blaustein and Lederer, 1999), favored when Na^+ rapidly enters through $Na_V1.5$ depolarizing the sarcolemma. As such, the reverse mode of NCX contributes some Ca^{2+} to the cytosol during the early systolic phase when L-type Ca^{2+} channels are also activated facilitating CICR. The consequent rise of cytosolic Ca^{2+} then reverts the NCX to Ca^{2+} extrusion or forward mode exchange, which contributes to muscle relaxation in diastole.

In CPVT, RyR2 channels aberrantly release SR Ca^{2+} during diastole when the cardiac action potential is in the late repolarization phase. At this point, a transient increase of inward I_{NCX} can generate DADs that may reach threshold to trigger an ectopic action potential which can lead to the characteristic bidirectional ventricular tachycardia of CPVT (Baltogiannis et al., 2019; Zhao et al., 2015b). Therefore, the activity of NCX is a key component in mediating the arrhythmic phenotype of CPVT and may provide an extra point of therapeutic control.

Flecainide's actions on NCX function may involve both direct and indirect effects. Kuroda et al. (2017) have recently reported an activating action of 30 µM flecainide on NCX. In the forward-Ca^{2+} export mode, this resulted in an ∼30% increased activity, which in the context of CPVT may permit more efficient removal of Ca^{2+}. However, the inward current would also be increased and may paradoxically pose a greater risk of triggering DADs. This would, of course, depend on cytosolic $[Na^+]$ and the temporal nature of I_{NCX} relative to $Na_V1.5$ channel recovery, the former of which is likely diminished by flecainide's inhibition of I_{Na}. It is also tempting to speculate that an enhanced NCX extrusion of Ca^{2+} may reduce its availability for reuptake by SERCA in turn reducing luminal $[Ca^{2+}]$ and therefore SR Ca^{2+} load. Although flecainide does not alter the total SR Ca^{2+} load (Watanabe et al., 2009), junctional SR Ca^{2+} load has not been specifically measured and could decrease if NCX is located in or close to dyadic regions (Scriven et al., 2000; Bovo et al., 2014). Such a decline would contribute to the reduced spark mass with flecainide (Watanabe et al., 2009; Hilliard et al., 2010). Elevated diastolic Ca^{2+} may also downregulate $Na_V1.5$ and therefore I_{Na} as demonstrated in the homozygous RyR2-P2328S$^{+/+}$ mouse (Ning et al., 2016). Here, Ca^{2+} as a second messenger can target a number of signaling pathways which could lead to diminished I_{Na} and thereby provide a further safety margin (Luo et al., 2017; Ning et al., 2016; Casini et al., 2009; Salvage et al., 2021b). Indirect effects of flecainide on NCX function are well recognized (Bannister et al., 2015; Sikkel et al., 2013; Steele et al., 2013) and arise from the direct inhibition of I_{Na} which in turn reduces cytosolic $[Na^+]$, and therefore the driving force for reverse mode Ca^{2+} influx. Consequently, an increased forward mode Ca^{2+} efflux would be favored, as observed at concentrations of flecainide (5 µM) within the therapeutic range (Sikkel et al., 2013). Undoubtedly, NCX is a major contributor to Ca^{2+} homeostasis. However, its precise contribution to normal function, CPVT and flecainide efficacy requires further investigation and likely depends on many variables including experimental parameters, experimental model (species), and the specific CPVT mutation.

General efficacy of class 1 Na^+ channel blockers in RyR2 inhibition and prevention of CPVT

Several studies have compared the efficacy of flecainide with that of other class 1C antiarrhythmic Na^+ channel blockers, in blocking RyR2 channels (Table 1) and in actions on Ca^{2+} waves and Ca^{2+} sparks (Table 2). To summarize, flecainide, R-propafenone, and S-propafenone produce a similar open state block to ∼20% of the maximum conductance. R-propafenone is the most effective channel blocker with an IC_{50} of 12 µM, compared to flecainide (16 µM) and S-propafenone (25 µM; Hwang et al., 2011). Flecainide and R-propafenone suppress Ca^{2+} wave parameters in permeabilized *CSQ2*$^{-/-}$ myocytes, with the highest potency (IC_{50} 2 and 12.8 µM, respectively) and efficacy. Other drugs (including S-propafenone) either have a lower potency and efficacy or are ineffective. Both flecainide and R-propafenone decreased Ca^{2+} spark mass and appeared to convert propagated Ca^{2+} waves into nonpropagated wavelets and frequent sparks (Hwang et al., 2011; Galimberti and Knollmann, 2011). Both flecainide and R-propafenone inhibit Ca^{2+} waves with significantly lower IC_{50} and higher efficacy in CPVT models (CSQ2$^{-/-}$ and the heterozygous RyR2-R4496C$^{+/-}$ mice) compared to WT models (Savio-Galimberti and Knollmann, 2015). In addition, both flecainide and R-propafenone are effective in reducing CPVT in animal models and in patients (Hwang et al., 2011).

Therapeutic concentrations of flecainide

The therapeutic range of flecainide is 0.2—1 mg/l (Valdes et al., 1998) equating to an upper limit of around 2 µM, a concentration which would favor its inhibitory actions on I_{Na} and I_{Kr} and largely preclude actions on current through the L-type Ca^{2+} channel (I_{CaL}), I_{NCX1}, and through RyR2. However, flecainide, due to its pKa ∼9.3, is 99% protonated at physiological pH (Liu et al., 2003). It is known to accumulate within the cell due to partitioning across the membrane (Melgari et al., 2015). It is then possible that local concentrations of flecainide within domains of the cytosol such as the dyadic space may be increased, although at first thought unlikely to reach levels associated with voltage-dependent block of isolated RyR2 channels in bilayers >5 µM (Mehra et al., 2014; Bannister et al., 2015; Salvage et al., 2021a). Since there is now general agreement that block of RyR2 Ca^{2+} leak does contribute to flecainide's antiarrhythmic efficacy in CPVT in conjunction with I_{Na} block and NCX activation (Steele et al., 2013; Salvage et al., 2018; Bannister et al., 2021; Yang et al., 2016; Kryshtal et al., 2021), either higher than predicted concentrations must exist within cellular microdomains, or intracellular factors increase RyR2 sensitivity to flecainide. Indeed, it is notable that a number of RyR2-active compounds in addition to flecainide act at lower concentrations in the cell than in the bilayer. For example, the IC_{50} for tetracaine inhibition of P_o is between 40 µM (Hilliard et al., 2010) and 426 µM (Watanabe et al., 2009; Laver and van Helden, 2011) and is suggested to be significantly reduced in intact myocytes (Shonts, 2011), where 25 µM tetracaine depresses Ca^{2+} waves (Venetucci et al., 2007). Similarly, caffeine induces Ca^{2+} waves at concentrations of 0.2–0.5 µM (Trafford et al., 2000; Venetucci et al., 2007)—concentrations at which

there is little effect on P_o in bilayers where the AC_{50} is 9.0 µM (Porta et al., 2011). It is likely that the cooperative nonlinear nature of CICR amongst clustered RyR2 during spark generation (see Fig. 7 and further discussion below) contributes to the higher efficacy of these compounds in myocytes.

Impact of the tetrameric nature of RyRs in flecainide's efficacy in CPVT

A further RyR2-mutation–specific consideration with flecainide's action is the impact of the tetrameric nature of the channel protein and whether a mutation is dominant or recessive. Most single-channel studies examine homozygous channels in which all four subunits are either WT or mutant. However, in heterozygote carriers, RyR2 channels are composed of WT and mutant subunits in five different combinations following a binomial distribution (Bongianino et al., 2017). The properties of an individual channel depend on the particular combination of subunits in that channel (Li and Chen, 2001; Bongianino et al., 2017; Zahradník et al., 2005). A simplistic assumption is that, with dominant mutations, the presence of one or more mutant subunits is sufficient to disrupt regulatory binding sites, keeping in mind that ∼6.5% of RyRs are likely to be WT homotetramers and 6.5% mutant homotetramers (Bongianino et al., 2017). On the other hand, recessive mutations only express the phenotype when all four subunits carry the mutation. The presence of different combinations of mutant and WT subunits will add to the complexity of interpreting the actions of flecainide in cellular models of dominant mutations. Interestingly as an alternative to drug therapy, Bongianino et al. (2017) found that the CPVT phenotype with the dominant R4496C mutation was reduced following the use of an siRNA that selectively silences mutant RyR2-R4496C mRNA, while not affecting the WT allele.

More unanswered questions

Is flecainide's RyR2 action in CPVT mutation-specific?

The efficacy of some drugs that reduce Ca^{2+} leak through RyR2 channels carrying CPVT mutations is mutation specific. For example, dantrolene, used clinically to reduce RyR1-mediated Ca^{2+} leak with N-terminal malignant hyperthermia mutations such as R615C, is also effectively antiarrhythmic in animal models of heart failure and CPVT (Walweel et al., 2017; Kobayashi et al., 2010). In CPVT patients, dantrolene is more effective with N-terminal and central domain mutations than mutations outside these regions and is ineffective with transmembrane mutations (Penttinen et al., 2015). The Rycal compound JTV519 reduces Ca^{2+} leak by stabilizing FKBP12.6 binding to RyR2 and is also more effective with N-terminal and central domain RyR2 mutations than with C-terminal mutations (Tateishi et al., 2009). It is therefore interesting that flecainide was initially reported ineffective in reducing spontaneous Ca^{2+} release events in heterozygous mice (RyR2-R4496C$^{+/-}$) carrying the transmembrane C-terminal RyR2-R4496C mutation (Liu et al., 2011). In contrast, flecainide did reduce spontaneous Ca^{2+} release in the CSQ2$^{-/-}$ mouse model (Watanabe et al., 2009). CSQ influences RyR2 activity through triadin and junctin interactions with luminal loops of RyR2 and also cytoplasmic regions outside the transmembrane/C-terminal domains (Groh et al., 1999; Beard et al., 2004; Györke et al., 2004; Li et al., 2015). Although flecainide was later found to be effective in reducing spontaneous Ca^{2+} release in RyR2-R4496C$^{+/-}$ under different experimental conditions (Hwang et al., 2019), the possibility remains that flecainide is less effective with C-terminal mutations.

The answer to mutation-specificity likely depends on whether the cellular efficacy of flecainide is RyR2 pore block, or whether the drug acts by binding to the protein cytoplasmic domains influencing channel gating by steric changes initiated at remote binding sites transmitted to pore gating mechanisms through intradomain, interdomain, and intersubunit interaction sites. In this latter case, the efficacy of flecainide could well depend on the location of the mutation site and how conformational changes associated with flecainide binding might interact with conformational changes induced by the mutation. On the other hand, if flecainide blocks Ca^{2+} release in vivo by binding in the channel pore then this simple blocking action might not depend on the mutation site.

Not unexpectedly, there is evidence that gain-of-function point mutations in *RyR1* and *RyR2* increase channel opening through a variety of mechanisms, consistent with the complex organization of these tetrameric multidomain ion channels (Iyer et al., 2022). The variety of possible mechanisms that would allow mutations in different domains to alter channel gating underlines the need for therapies targeted to mutations in particular domains of the protein (Dulhunty, 2022; Dulhunty et al., 2022; Iyer et al., 2022).

We next consider potential broad mechanisms leading to increased Ca^{2+} leak with three CPVT models, the homozygous CSQ2 knockout (*CSQ2*$^{-/-}$) mouse, the heterozygous RyR2-R4496C$^{+/-}$, and homozygous RyR2-P2328S$^{+/+}$ mouse, with mutations located in, or influencing, different RyR2 domains and likely mechanisms for reported actions of flecainide. However, as far as we can ascertain with PubMed searches, P2328S is the only *RyR2* mutation examined with flecainide at a single channel level (Fig. 6; Salvage et al., 2021a; Dulhunty et al., 2022).

The CSQ2 knockout mutation. The most complex situation from a mechanistic perspective is CSQ2 knockout, where the effect of the mutation on RyR2 is secondary to the lack of CSQ2 binding to other members of the RyR2 complex and to substantial changes in Ca^{2+} buffering and dynamics (Faggioni et al., 2012; Kornyeyev et al., 2012). CSQ2 inhibits RyR2 by binding to RyR2-associated transmembrane proteins triadin and junctin, which in turn interact with luminal and cytoplasmic RyR domains (Groh et al., 1999; Beard et al., 2002, 2004; Györke et al., 2004; Li et al., 2015). CSQ2, triadin, and junctin contribute independently and together to cardiac EC coupling (Györke and Terentyev, 2008; Knollmann, 2009; Altschafl et al., 2011; Cai et al., 2012). Reduced triadin and calsequestrin levels contribute to CPVT (Cacheux et al., 2020). Triadin and junctin bind to luminal loops of RyR2 which are continuous with the transmembrane helices and channel gating mechanisms. Consequently, structural changes in the two proteins due to CSQ2 depletion may be transmitted through the binding sites to alter

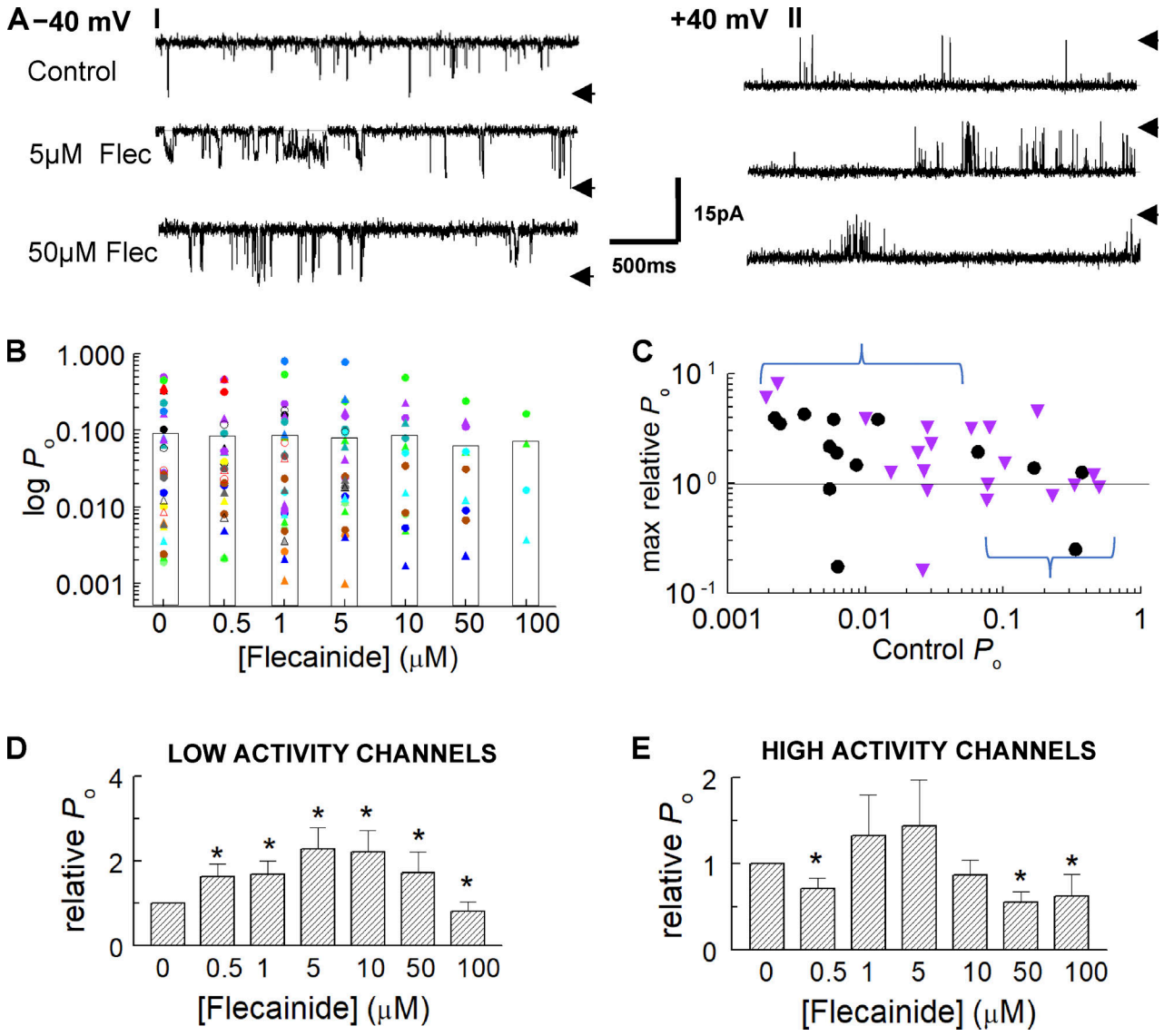

Figure 6. **Significant voltage-independent activation of low activity P2328S channels observed with flecainide concentrations of 0.5 to 50 μM, while inhibition of high-activity channels was less consistent than in WT channels.** Related to Fig. 3. Data is shown for single RyR2 channels (Salvage et al., 2021a). **(A)** Representative channel currents before addition of flecainide (upper) and with 5 μM flecainide (middle) and 50 μM flecainide (lower) at −40 mV, with channel opening downward (A, I) and +40 mV, with channel opening upward (A, II). Arrows indicate maximum open current level. **(B)** Individual relative P_o data at +40 mV (circles) and −40 mV (triangles). Data for each channel is represented by symbols of the same color. The data in this graph illustrates the voltage independence of changes with flecainide and suggests a decline in activity as flecainide concentration increases in channels with high control P_o values, in contrast to an increase in activity in channels with a lower control P_o. The boxes indicate the average P_o for each flecainide concentration. **(C)** Individual maximum relative P_o values with flecainide, plotted against control P_o. Black circles, +40 mV; purple triangles, −40 mV. Maximum relative P_o is the highest value recorded over 60–90 s segments of activity with flecainide in each channel across all concentrations of the drug. Values below 1 indicate that there was no increase in activity at any concentration, but do not reflect the full decline in activity. The full decline in activity in individual channels is shown in B. **(C–E)** The upper opening bracket and arrow indicates channels included in the low control activity group (D), while the lower closing bracket and arrow indicate channels included in the high control activity group (E). The control P_o dependence of relative P_o seen in WT channels (Fig. 3) was not apparent in the P2328S channels. Nevertheless, the P2328S data was separated into low activity (P_o < 0.08) and high activity (P_o > 0.08) groups for comparison with WT channel data. D and E show average relative P_o values for low- (D) and high-activity (E) channels at individual flecainide concentrations. The low-activity channels show significant increases in activity with 0.5–50 μM flecainide and a small but significant decline with 100 μM flecainide. The high-activity P2328S channels show a less consistent decline in P_o when compared with that in WT channels (Fig. 3). Single-channel traces and graphs are from Salvage et al. (2021a).

RyR2 luminal loop conformation and impact channel gating. Similarly, the cytoplasmic binding sites for triadin and junctin may be structurally impacted by loss of CSQ2 binding. Such structural changes could be communicated to the distant pore via steric changes in intradomain and interdomain interactions along the molecular pathway from the binding site to the pore. The absence of CSQ2 results in CPVT and spontaneous Ca^{2+}-release events (Knollmann et al., 2006; Watanabe et al., 2009). Flecainide prevents CPVT in *CSQ2*$^{-/-}$ mice by reducing Ca^{2+} waves, indicating that inhibition of RyR2 activity contributes to

flecainide's efficacy (Watanabe et al., 2009; Yang et al., 2016; Hwang et al., 2019; Kryshtal et al., 2021). Flecainide could reduce Ca^{2+} leak by either blocking the counter current flow through RyR2 and/or by binding to inhibitory sites on the cytoplasmic domain of the protein, where its precise action could be mutation specific if its binding site overlaps with the triadin or junctin binding site. In addition to the effects of altering interactions between triadin, junctin, and RyR2, the absence of CSQ2 alters the Ca^{2+}-buffering capacity of the SR, increasing the rate of SR refilling and reducing refractory periods (Faggioni et al., 2012; Kornyeyev et al., 2012).

The R4496C mutation. R4496 is located near the junction between the central and transmembrane domains of RyR2 in a region critical in transmitting signals arising in the cytoplasmic domains to the S6 helix and channel pore (Peng et al., 2016). The effect of substituting positively charged arginine residues with neutral cysteine residues could disrupt local structure by removing the ionic interactions involving the positively charged residue, as predicted for the D3638A mutation (Acimovic et al., 2018). The functional effect of R4496C on RyR2 activity is controversial. Homozygous mutant channels expressed in HEK293 cells show enhanced basal activity (Jiang et al., 2002), and heterozygous mouse RyR2-R4496C$^{+/-}$ myocytes demonstrate increased RyR2 Ca^{2+} sensitivity for diastolic Ca^{2+} release, Ca^{2+} waves, and triggered activity (Fernández-Velasco et al., 2009). However, other evidence attributes Ca^{2+} waves to elevated SR Ca^{2+} content, rather than reduced RyR2 thresholds for Ca^{2+} release (Kashimura et al., 2010). As with other CPVT mutations, there are reports that flecainide reduces CPVT through blocking I_{Na} as well as RyR2 (Liu et al., 2011; Hwang et al., 2019). The location of R4496, in the most C-terminal of the three hotspot regions for gain-of-function *RyR2* mutations, is close to a number of LOF mutations (Priori et al., 2021; Olubando et al., 2020). Therefore, the R4496C mutation may impact on nearby inhibitory interactions that compromise experimental results and conclusions about the effects of both the mutation and the action of flecainide. Indeed, Jiang et al. (2007) show that the R4496K substitution enhanced basal P_o while R4496E depressed basal P_o, suggesting the charge and polarity at residue 4496 plays an essential role in RyR2 channel gating. Again, there is no evidence to indicate whether flecainide's pore block or direct binding mechanism are most likely to contribute to its efficacy. It will be important to establish the effect of both the mutation and of flecainide on RyR2 channel activity.

The P2328S mutation. P2328S is a mutation located in RyR2 helical domain 1 (HD1; Peng et al., 2016; Dhindwal et al., 2017; Bauerová-Hlinková et al., 2020) in the second of three hot-spot regions for CPVT mutations (Priori et al., 2021; Olubando et al., 2020). The pathways for transmission of the local structural effects of the mutation from HD1 through to the channel pore in the distant transmembrane domain may well follow a similar route through the central and C-terminal domains to that elegantly shown for the malignant hyperthermia R615C mutation in RyR1 (Woll et al., 2021; Iyer et al., 2020). The local structural effect of the proline to serine substitution could be significant as proline is known to have a strong structural influence and to interrupt helices, introducing a kink in the helix and changing its direction. Thus, its substitution by a serine could reverse the influence of the proline residue on the native structure in the HD1 region in the WT protein.

The RyR2 P2328S mutation is one of a few CPVT mutations associated with both atrial and ventricular fibrillation (Zhang et al., 2011). Increased cytoplasmic Ca^{2+} sensitivity was seen after PKA phosphorylation and reduced FKBP binding of P2328S channels expressed in HEK293 cells (Lehnart et al., 2004). Hearts of P2328S mice show a reduced action potential conduction velocity, reduced $Na_V1.5$ expression, and Na^+ channel function with increased RyR2 sensitivity to cytoplasmic Ca^{2+} and DADs (Zhang et al., 2013; King et al., 2013; Salvage et al., 2015; Ning et al., 2016; Goddard et al., 2008). The RyR2 channels show a left shift in their cytoplasmic Ca^{2+} activation curves and an unexpected left shift in Ca^{2+} inactivation, involving $[Ca^{2+}]_i$ approaching systolic $[Ca^{2+}]_i$ (Salvage et al., 2019), and approaching the higher affinity Ca^{2+} inactivation in skeletal RyR1 channels. These changes were not associated with excess phosphorylation or reduced FKBP12 binding (Salvage et al., 2019).

Flecainide was proarrhythmic in WT but paradoxically antiarrhythmic in homozygous, RyR2-P2328S$^{+/+}$ atria (Salvage et al., 2015). The increased arrhythmic incidences in WT atria accompanied a reduced I_{Na} with a consequent reduction of conduction velocity. The reduced arrhythmia in such P2328S atria was explained by flecainide's block of RyR2 lowering the mutation-induced high cytoplasmic $[Ca^{2+}]$ and thus reducing DAD-induced arrhythmogenic action potential activity (Salvage et al., 2015). The lower $[Ca^{2+}]_i$ would relieve Ca^{2+}-dependent inhibition of I_{Na}, although flecainide would at the same time inhibit I_{Na}. Unexpectedly and again paradoxically, the direct effect of flecainide on P2328S channels was to suppress voltage-independent inactivation in higher activity channels (Fig. 6; Salvage et al., 2021a; Dulhunty et al., 2022). In contrast to WT channels, low activity P2328S channels were significantly activated at flecainide concentrations from 0.5 to 50 µM, although significantly inhibited by 100 µM flecainide (Fig. 6). These changes may suggest that one or both peripheral flecainide binding sites are in the vicinity of the peripheral P2328 residue and influenced by structural changes induced by the P2328S mutation. Overall, there are clearly several unexplained actions of flecainide on WT and P2328S RyR2 channels that remain to be fully addressed, as well as the particular flecainide actions on RyR2 that are invoked in the observed cellular changes.

Can CICR nonlinearities contribute to flecainide-induced reduction in spark mass and wave frequency?

It is not clear why flecainide in myocytes induces an increase in spark frequency but a decreased spark mass and wave frequency (Watanabe et al., 2009; Hilliard et al., 2010). Hilliard et al. (2010) suggest that the increased spark frequency may be due to the effect of flecainide in reducing spark mass. Each spark results in a smaller reduction in SR luminal $[Ca^{2+}]$, so that smaller spontaneous sparks occur more frequently due to a luminal Ca^{2+} regulation mechanism that maintains a constant Ca^{2+} influx via SERCA. One alternative explanation, among others, is that the spark rate is increased because of the voltage-independent activation of RyR2 by flecainide (Salvage et al., 2021a) and

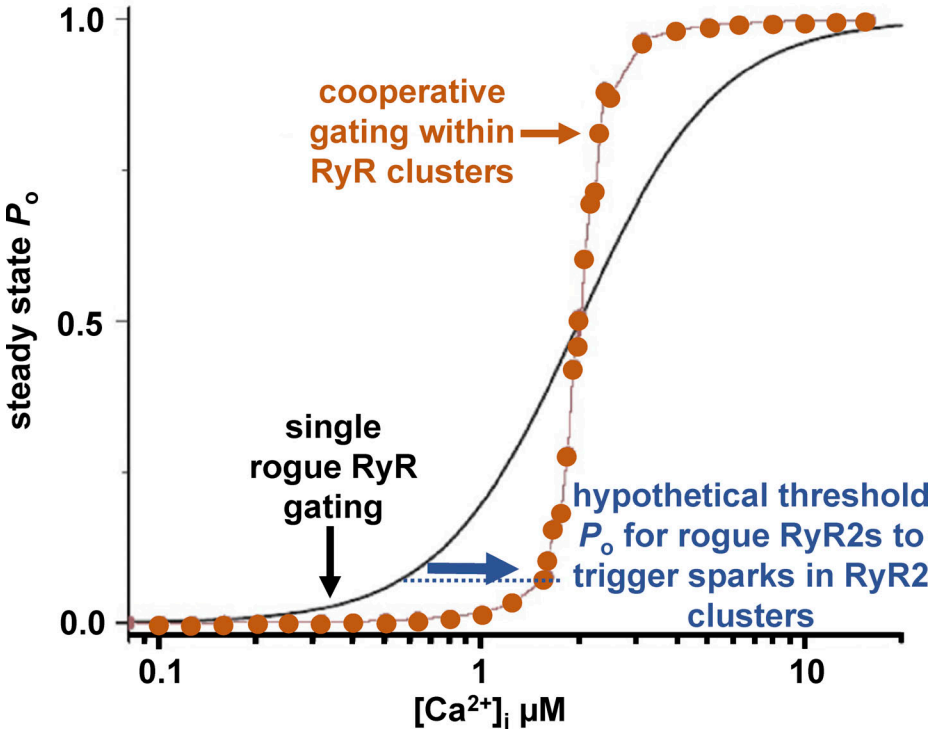

Figure 7. **Cooperative gating between as few as eight coupled RyR2s in a dyadic junction (couplon) dramatically increases the steepness of the predicted relationship between P_o and $[Ca^{2+}]_i$.** The solid black line shows the predicted P_o versus $[Ca^{2+}]_i$ relationship for a single or rogue nonjunctional RyR2. The filled brown circles show the relationship predicted for eight cooperatively gated coupled junctional RyR2s. As a consequence of cooperativity, P_o of nonjunctional rogue RyR2s increase as $[Ca^{2+}]_i$ increases through much of the diastolic range, concentrations which have little effect on P_o of the clustered RyR2s. The graph shows predicted effects of changing $[Ca^{2+}]_i$ on P_o. The P_o and $[Ca^{2+}]_i$ values are within the physiological range but have not been experimentally verified in vivo because the technology to do so does not yet exist. The figure is modified from Fig. 2 of Sobie et al. (2006) under copyright license 1210751-1.

flecainide-stabilized substate activity (Figs. 3, 4, and 6). This could cause a local depletion of SR Ca^{2+} which would in turn lead to an abbreviated spark to maintain a constant uptake-leak balance. It is possible, given the complex and variable geometry of couplons (Walker et al., 2015; Chen et al., 2018), and the multiple flecainide binding sites on RyR2 (Salvage et al., 2021a), that both activation and inhibition of RyRs can overlap during diastole. However, the overall effect is inhibition of spark mass and wave frequency. It is likely that cooperative gating between RyRs in clusters (Fig. 7) leads to a steeper inhibitory effect in vivo than that experienced by individual RyRs in bilayers or rogue nonjunctional RyRs.

The molecular basis for the reduced occurrence of diastolic Ca^{2+} waves in the presence of flecainide is similarly speculative, but is likely to be related to RyR2 activity and CICR which underlie spark formation and thus related to propagating Ca^{2+} waves which arise from the stationary Ca^{2+} sparks (Hoang-Trong et al., 2021). It follows that the reduction in spark mass with flecainide could reduce the probability of a spark activating release events at neighboring couplons to generate propagating waves (Hilliard et al., 2010). However, the relationship between sparks and waves is not straightforward and it is likely that rogue RyRs in regions between clusters at release sites are required for propagation (Chen et al., 2018; Hoang-Trong et al., 2021). A steep inhibitory effect on spark mass due to cooperativity within clusters would contribute to the reduced probability of sparks activating neighboring couplons, although this would be counteracted by the less steep inhibitory effect on Ca^{2+} release from nonjunctional rogue RyR2 channels (Fig. 7).

Does flecainide reduce Ca^{2+} leak from the SR and what is the impact of cooperativity?

A decline in Ca^{2+} leak was initially measured in the $CSQ2^{-/-}$ myocytes in conjunction with the increased event frequency and reduced spark mass and wave occurrence, but without any change in total SR Ca^{2+} content (Watanabe et al., 2009). Later calculations of leak based on spark mass and frequency suggested that flecainide did not alter either spark leak or total SR Ca^{2+} content (Hilliard et al., 2010). Conversely, investigations using the RyR2-P2328S mouse model, as well as simulation predictions, suggested that flecainide does inhibit Ca^{2+} leak (Salvage et al., 2015; Curran and Louch, 2015; Lehnart and Lederer, 2010). The different conclusions could arise from the nature of the $CSQ2^{-/-}$ and homozygous RyR2-$P2328S^{+/+}$ mutations, due to effects of CSQ2 removal in $CSQ2^{-/-}$ myocytes on both SR Ca^{2+} buffering and Ca^{2+} availability. In addition, conclusions about leak based on total SR $[Ca^{2+}]$ may not reveal changes in $[Ca^{2+}]$ in junctional microdomains of the SR which are mainly responsible for generating sparks. Indeed, the characteristics of leak and effects on SR Ca^{2+} may differ in junctional and nonjunctional microdomains as discussed below and thus

confound conclusions about leak based on total SR Ca^{2+} content. Nonjunctional SR occupies a similar or larger volume than junctional SR (Jorgensen and McGuffee, 1987) and can contribute substantially to Ca^{2+} leak (Santiago et al., 2010; Chen et al., 2018). Indeed, Ca^{2+} leak due to spark activity is not necessarily a reflection of overall leak, which is strongly influenced by both clustered RyRs and rogue RyRs, where P_o can be higher than normal but below triggering threshold (Santiago et al., 2010; Chen et al., 2018).

A further related consideration is that flecainide may alter Ca^{2+} leak from junctional and nonjunctional SR and produce associated changes in local SR $[Ca^{2+}]$ in opposing ways. This difference depends on RyR clustering and cooperativity in junctions as opposed to individual or loosely coupled nonjunctional RyRs. As a result of cooperativity, the increase in P_o with $[Ca^{2+}]_i$ predicted for individual RyRs becomes very steep for clustered RyRs during spark generation (Stern et al., 1999; Sobie et al., 2006; Cheng and Lederer, 2008; Fig. 7). Flecainide inhibition of Ca^{2+} release would reduce the dyadic $[Ca^{2+}]_i$ and P_o/CICR would decline steeply thus reducing spark mass and spark leak. This alone could increase couplon SR $[Ca^{2+}]$ as less Ca^{2+} is released with each spark. However, this increase would be opposed by increased spark frequency, resulting in a constant dyadic SR $[Ca^{2+}]$ if the relationship between mass and frequency is tightly controlled, which although indicated (Hilliard et al., 2010), has not been conclusively demonstrated. Any increase in dyadic SR Ca^{2+} content might be masked in a measure of total Ca^{2+} load by the response of nonjunctional SR where a decline in $[Ca^{2+}]_i$ with flecainide inhibition has a much smaller effect on P_o and Ca^{2+} leak (Fig. 7), so that a pump/leak balance can be maintained. In addition, changes in SR $[Ca^{2+}]$ associated with sparks would be transient and unsynchronized across the myocyte and may not be detected in the measurement of total SR $[Ca^{2+}]$.

Cooperativity may contribute to the opposing effects of flecainide in increasing spark frequency while reducing spark mass. Nonjunctional RyRs are predicted to be activated at a lower $[Ca^{2+}]_i$ than junctional RyRs over much of the diastolic $[Ca^{2+}]_i$ range (Fig. 7). Indeed, junctional RyRs on the edge of a cluster may have $[Ca^{2+}]_i$ sensitivities intermediate between those of individual and fully clustered RyRs and thus be activated by lower Ca^{2+} than RyRs in the center of a cluster (Walker et al., 2015; Chen et al., 2018). Predictions and experimental data suggest nonjunctional or loosely coupled rogue RyRs can trigger sparks with levels of cytoplasmic and luminal $[Ca^{2+}]$ that are likely to exist in vivo under steady state conditions (~0.1 μM and ~0.6–1.0 mM, respectively; Chen et al., 2018). When flecainide inhibits RyR2, channel open times are reduced and closures prolonged (Mehra et al., 2014; Salvage et al., 2021a), so that P_o falls and leak is reduced. Consequently, it is conceivable that $[Ca^{2+}]_i$ enters a range in which edge and central RyRs and possibly some nonjunctional RyRs can trigger sparks, albeit with a lower mass than would be seen at higher $[Ca^{2+}]_i$ where smaller sparks merge into larger compound sparks (Cheng et al., 1996).

How might subconductance activity impact on Ca^{2+} sparks and Ca^{2+} waves?

Stabilization of intrinsic substate activity by flecainide is shown in records in Figs. 3 A, 4, and 6. It is notable in these records that openings to the full conductance either remain constant or decrease as the subconductance openings increase. Thus the subconductance would contribute to the voltage-independent increase in P_o seen in low activity channels where P_o was measured with a threshold discriminator set close to the baseline at ~2 pA (Salvage et al., 2019) and would be better reflected in a measure of mean current which is not dependent on a threshold discriminator (Gallant et al., 2004). With low amplitude substate openings, the mean current increases more than the measured P_o, because the openings are close to the baseline and not detected with a 2-pA discriminator (Figs. 3 and 4). The many larger substate openings to levels up to ~50% would not contribute to P_o measured using a 50% discriminator (e.g., Mehra et al., 2014), but would contribute to the current flowing through the channel and to Ca^{2+} leak and the observed increase in the probability of spark generation (Hilliard et al., 2010). However, the spark mass may decrease due to the reduced contribution from full conductance openings, depending on the relative contribution of full and substate openings to the total current under cellular conditions. Whether this would be proarrhythmic or antiarrhythmic depends on the spark–wave relationship and the even more complex wave–DAD relationship in the cell, as discussed above.

In contrast to the flecainide-stabilized substate, the flecainide-induced substate (Fig. 1) occurs only when flecainide blocks the channel—it is not a flecainide-independent opening of the channel. Thus, the reduction in current flowing through the channel would be proportional to the decline in P_o measured with a 50% discriminator (Watanabe et al., 2009; Hilliard et al., 2010; Mehra et al., 2014; Kryshtal et al., 2021), but less than predicted if the channel closed fully. Consistent with this is the smaller decline in P_o reported by Bannister et al. (2015) using a model-dependent assessment of P_o (Fig. 1). The antiarrhythmic effect of flecainide in reducing the leak through RyR2 would be reduced by closures to the substate level.

Flecainide's efficacy in arrhythmogenic LOF RyR2 mutations

LOF RyR2 mutations have been included as genetic variants of CPVT (Priori et al., 2021). They should perhaps be considered a separate familial RyR2-dependent, noncatecholaminergic arrhythmic syndrome. Indeed, many LOF mutants linked to sudden cardiac death or aborted cardiac death do not respond to exercise stress testing or produce the characteristic bidirectional ventricular tachycardia, hallmarks of CPVT (Sun et al., 2021; Zhong et al., 2021; Ormerod et al., 2021). Instead LOF mutations lead to a CRDS, in which the general effect of the mutations on RyR2 is to reduce or abolish CICR indicated in $[^3H]$ ryanodine binding and single channel experiments (Zhao et al., 2015a; Zhao et al., 2015b; Jiang et al., 2007; Hirose et al., 2021).

At the cellular level, cells expressing these mutations lack detectable Ca^{2+} oscillations and display a reduced sensitivity to caffeine and store-overload–induced Ca^{2+} release (SOICR), suggesting they may not respond as fully to β-adrenergic stimulation (Ormerod et al., 2021; Sun et al., 2021; Hirose et al., 2021; Zhao et al., 2015b; Fujii et al., 2017). SR Ca^{2+} content may be increased because of the lack of SOICR. When SOICR is initiated, it terminates more slowly in the mutant with a greater release of

Ca^{2+}, exacerbated by an increased SR Ca^{2+} content. Therefore, Ca^{2+} transients may be increased particularly after a long burst and a long pause protocol, which would simulate the recovery period after exercise, and was used to induce early afterdepolarisation (EAD) and lead to ventricular arrhythmia. EADs are, like DADS, generated by electrogenic NCX activity initiated by the larger than normal Ca^{2+} transients (Priori et al., 2021; Sun et al., 2021).

A recent study identified a potential inverse relationship between the severity of the clinical phenotype and the level of impaired SR Ca^{2+} release (Hirose et al., 2021). Two of the mutations (E4146D and S4938F) rendered the channel less active, but still functional, resulting in impaired Ca^{2+} waves and an absence of Ca^{2+} oscillations with a severe clinical phenotype of QT prolongation, short-coupled PVC, and ventricular fibrillation. In contrast, the other two mutations (S4168P and K4594Q) rendered the channels almost completely nonfunctional with an absence of both Ca^{2+} oscillations and Ca^{2+} waves, yet clinically only QT prolongation and mild arrhythmias were observed (Hirose et al., 2021). This surprising finding suggests a complete loss of function may be less harmful than merely reduced function. However, mouse models indicate that homozygous expression of LOF mutants is embryonically lethal (Zhao et al., 2015b; Sun et al., 2021) and so the in vivo complexity of mixed populations of WT and mutant homo- and heterotetrameric RyR2 channels along with potential compensatory mechanisms is not accounted for (Santiago and Priori, 2021). In two separate family pedigrees, harboring either the D4646F or the A4142T LOF mutations, phenotypes varied in severity ranging from sudden cardiac death and aborted sudden cardiac death to being asymptomatic (Sun et al., 2021; Ormerod et al., 2021). Furthermore, in the heterozygous RyR2-D4646F$^{+/-}$ mouse, I_{CaL} was upregulated (Sun et al., 2021), likely as a result of reduced Ca^{2+} inhibition. In addition to altered L-type Ca channel function, further ion channel remodeling was also observed with increased density of $I_{Na/Ca}$ and transient outward K^+ current (I_{To}), collectively these alterations likely act to maintain a level of Ca^{2+} cycling sufficient to maintain EC coupling.

Despite the cellular and clinical phenotype differing from that of CPVT, flecainide is also effective in preventing arrhythmia in human CRDS subjects with the heterozygous RyR2-A4142T$^{+/-}$ mutation and in the heterozygous RyR2-D4646F$^{+/-}$ mouse (Ormerod et al., 2021; Sun et al., 2021). The effect of flecainide on single channels with these mutations has not been reported. However, there are several possible actions. If flecainide exerted its usual inhibitory effect on RyR2, then a reduction of the large Ca^{2+} release during longer SOICR events should be antiarrhythmic. However, it is counterintuitive that an inhibitory agent acting on a channel that is presumably not Ca^{2+} activated, would be antiarrhythmic. Alternatively, flecainide could be exhibiting its voltage-independent activating action in these channels which are likely to have very low P_o prior to flecainide addition (Salvage et al., 2021a; Dulhunty et al., 2022). Activation could potentially restore the normal diastolic P_o and reduce the build-up of SR Ca^{2+} load. These contrasting actions of flecainide on RyR2 may be compounded by the degree of RyR2 inhibition exhibited by different mutations as indicated by Hirose et al. (2021). It is also possible that the effects are due to flecainide's classical block of $Na_V1.5$, so that the infrequent but dramatic arrhythmogenic release of Ca^{2+} has a reduced ability to induce EADs because the electrogenic effect of Na entry through NCX would be mitigated by the reduced Na^+ entry through $Na_V1.5$. Finally, a direct effect of flecainide on NCX should also be considered, though the extent to which this may contribute is not presently clear and warrants further investigation, particularly as an increased $I_{Na/Ca}$ has been identified in a mouse model of CRDS (Sun et al., 2021). Clearly, this is another facet of the flecainide story that will be clarified in future studies.

Conclusions

Flecainide is used effectively to treat CPVT-related arrhythmia and has been shown to reduce Ca^{2+} leak through RyR2 during diastole in animal CPVT models, although the mechanisms of its therapeutic clinical efficacy are not well understood. The drug directly influences $Na_V1.5$, RyR2, and NCX activity. All three of these proteins are intimately involved in cardiac EC coupling and show interdependent functions. The overall efficacy of the drug in CPVT likely depends on the combined outcomes of the changes that it exerts either directly or indirectly on each of these proteins. Flecainide increases NCX activity, but the binding site is currently structurally and functionally uncharacterized. The single binding site for flecainide in the $Na_V1.5$ pore blocks the channel and is well characterized both structurally and functionally. In marked contrast, flecainide binding to the giant RyR2 protein is complex, with at least four separate inhibitory binding sites and one activation site in the protein suggested by the functional effects of the drug on single-channel activity. None of these binding sites have been specifically located in the linear sequence of RyR2 or on the high-resolution protein structure. However, the voltage-dependence of three of the inhibitory sites indicates that they are located in the pore or transmembrane assembly.

The effect of flecainide binding to these sites is to reduce current flow in the opposite direction to that of physiological Ca^{2+} fluxes. This suggests that the cellular action of flecainide binding to these sites might not be on Ca^{2+} efflux directly, but that it could also be a block of the counter ion current that flows through the pore to prevent SR membrane potential changes during the massive Ca^{2+} efflux during systole. The other two sites are not voltage-dependent and thus further from the pore and most likely located on the massive cytoplasmic domains of the RyR2 protein. Flecainide binding to one of these sites inhibits RyR2 activity and may contribute to the clinical efficacy of the drug which depends on an overall reduction in RyR2 activity. The second site supports a higher affinity increase in channel activity that could contribute to the occasionally observed proarrhythmic actions of flecainide, and possibly even to the antiarrhythmic mechanism in CRDS.

Acknowledgments

David A. Eisner served as editor.

The work was supported by grants to A.F. Dulhunty from the Australian National Health and Medical Research Council

(APP108477 to A.F. Dulhunty), to C.L.-H. Huang from the Medical Research Council (MR/M001288/1), the Wellcome Trust (105727/Z/14/Z) and British Heart Foundation (PG/14/79/31102 and PG/15/12/31280), and the Isaac Newton Trust/Wellcome Trust ISSF/University of Cambridge Joint Research Grants Scheme (to J.A. Fraser).

The authors declare no competing financial interests.

Author contributions: S.C. Salvage, C.L.-H. Huang, J.A. Fraser, and A.F. Dulhunty made substantial contributions conceptuulisation, writing and critical evaluation of the manuscript.

References

Acimovic, I., M.M. Refaat, A. Moreau, A. Salykin, S. Reiken, Y. Sleiman, M. Souidi, J. Přibyl, A.V. Kajava, S. Richard, et al. 2018. Post-translational modifications and diastolic calcium leak associated to the novel RyR2-D3638A mutation lead to CPVT in patient-specific hiPSC-derived cardiomyocytes. *J. Clin. Med.* 7:E423. https://doi.org/10.3390/jcm7110423

Ahern, G.P., P.R. Junankar, and A.F. Dulhunty. 1997. Subconductance states in single-channel activity of skeletal muscle ryanodine receptors after removal of FKBP12. *Biophys. J.* 72:146–162. https://doi.org/10.1016/S0006-3495(97)78654-5

Ahern, C.A., A.L. Eastwood, D.A. Dougherty, and R. Horn. 2008. Electrostatic contributions of aromatic residues in the local anesthetic receptor of voltage-gated sodium channels. *Circ. Res.* 102:86–94. https://doi.org/10.1161/circresaha.107.160663

Altschafl, B.A., D.A. Arvanitis, O. Fuentes, Q. Yuan, E.G. Kranias, and H.H. Valdivia. 2011. Dual role of junctin in the regulation of ryanodine receptors and calcium release in cardiac ventricular myocytes. *J. Physiol.* 589:6063–6080. https://doi.org/10.1113/jphysiol.2011.215988

Anderson, J.L., E.M. Gilbert, B.L. Alpert, R.W. Henthorn, A.L. Waldo, A.K. Bhandari, R.W. Hawkinson, and E.L. Pritchett. 1989. Prevention of symptomatic recurrences of paroxysmal atrial fibrillation in patients initially tolerating antiarrhythmic therapy. A multicenter, double-blind, crossover study of flecainide and placebo with transtelephonic monitoring. Flecainide Supraventricular Tachycardia Study Group. *Circulation.* 80:1557–1570. https://doi.org/10.1161/01.cir.80.6.1557

Apostolakis, S., M. Oeff, U. Tebbe, L. Fabritz, G. Breithardt, and P. Kirchhof. 2013. Flecainide acetate for the treatment of atrial and ventricular arrhythmias. *Expert Opin. Pharmacother.* 14:347–357. https://doi.org/10.1517/14656566.2013.759212

Baltogiannis, G.G., D.N. Lysitsas, G. di Giovanni, G. Ciconte, J. Sieira, G. Conte, T.M. Kolettis, G.B. Chierchia, C. de Asmundis, and P. Brugada. 2019. CPVT: Arrhythmogenesis, therapeutic management, and future perspectives. A brief review of the literature. *Front. Cardiovasc. Med.* 6:92. https://doi.org/10.3389/fcvm.2019.00092

Bannister, M.L., N.L. Thomas, M.B. Sikkel, S. Mukherjee, C. Maxwell, K.T. MacLeod, C.H. George, and A.J. Williams. 2015. The mechanism of flecainide action in CPVT does not involve a direct effect on RyR2. *Circ. Res.* 116:1324–1335. https://doi.org/10.1161/circresaha.116.305347

Bannister, M.L., A. Alvarez-Laviada, N.L. Thomas, S.A. Mason, S. Coleman, C.L. du Plessis, A.T. Moran, D. Neill-Hall, H. Osman, M.C. Bagley, et al. 2016. Effect of flecainide derivatives on sarcoplasmic reticulum calcium release suggests a lack of direct action on the cardiac ryanodine receptor. *Br. J. Pharmacol.* 173:2446–2459. https://doi.org/10.1111/bph.13521

Bannister, M.L., K.T. MacLeod, and C.H. George. 2021. Moving in the right direction: Elucidating the mechanisms of interaction between flecainide and the cardiac ryanodine receptor. *Br. J. Pharmacol.* 179:2558–2563. https://doi.org/10.1111/bph.15718

Bauerová-Hlinková, V., D. Hajdúchová, and J.A. Bauer. 2020. Structure and function of the human ryanodine receptors and their association with myopathies-present state, challenges, and perspectives. *Molecules.* 25:E4040. https://doi.org/10.3390/molecules25184040

Beard, N.A., M.M. Sakowska, A.F. Dulhunty, and D.R. Laver. 2002. Calsequestrin is an inhibitor of skeletal muscle ryanodine receptor calcium release channels. *Biophys. J.* 82:310–320. https://doi.org/10.1016/S0006-3495(02)75396-4

Beard, N.A., D.R. Laver, and A.F. Dulhunty. 2004. Calsequestrin and the calcium release channel of skeletal and cardiac muscle. *Prog. Biophys. Mol. Biol.* 85:33–69. https://doi.org/10.1016/j.pbiomolbio.2003.07.001

Bers, D.M. 2000. Calcium fluxes involved in control of cardiac myocyte contraction. *Circ. Res.* 87:275–281. https://doi.org/10.1161/01.res.87.4.275

Bers, D.M. 2001. Excitation-Contraction Coupling and Cardiac Contractile Force. Vol. 237. Springer, New York.

Bezanilla, F. 2008. How membrane proteins sense voltage. *Nat. Rev. Mol. Cell Biol.* 9:323–332. https://doi.org/10.1038/nrm2376

Bhat, M.B., S.M. Hayek, J. Zhao, W. Zang, H. Takeshima, W.G. Wier, and J. Ma. 1999. Expression and functional characterization of the cardiac muscle ryanodine receptor Ca^{2+} release channel in Chinese hamster ovary cells. *Biophys. J.* 77:808–816. https://doi.org/10.1016/S0006-3495(99)76933-X

Blaustein, M.P., and W.J. Lederer. 1999. Sodium/calcium exchange: Its physiological implications. *Physiol. Rev.* 79:763–854. https://doi.org/10.1152/physrev.1999.79.3.763

Bongianino, R., M. Denegri, A. Mazzanti, F. Lodola, A. Vollero, S. Boncompagni, S. Fasciano, G. Rizzo, D. Mangione, S. Barbaro, et al. 2017. Allele-specific silencing of mutant mRNA rescues ultrastructural and arrhythmic phenotype in mice carriers of the R4496C mutation in the ryanodine receptor gene (RYR2). *Circ. Res.* 121:525–536. https://doi.org/10.1161/circresaha.117.310882

Bovo, E., P.P. De Tombe, and A.V. Zima. 2014. The role of dyadic organization in regulation of sarcoplasmic reticulum Ca^{2+} handling during rest in rabbit ventricular myocytes. *Biophys. J.* 106:1902–1909. https://doi.org/10.1016/j.bpj.2014.03.032

Cacheux, M., J. Fauconnier, J. Thireau, A. Osseni, J. Brocard, N. Roux-Buisson, J. Brocard, J. Fauré, A. Lacampagne, and I. Marty. 2020. Interplay between triadin and calsequestrin in the pathogenesis of CPVT in the mouse. *Mol. Ther.* 28:171–179. https://doi.org/10.1016/j.ymthe.2019.09.012

Cai, W.F., T. Pritchard, S. Florea, C.K. Lam, P. Han, X. Zhou, Q. Yuan, S.E. Lehnart, P.D. Allen, and E.G. Kranias. 2012. Ablation of junctin or triadin is associated with increased cardiac injury following ischaemia/reperfusion. *Cardiovasc. Res.* 94:333–341. https://doi.org/10.1093/cvr/cvs119

Casini, S., A.O. Verkerk, M.M.G.J. van Borren, A.C.G. van Ginneken, M.W. Veldkamp, J.M.T. de Bakker, and H.L. Tan. 2009. Intracellular calcium modulation of voltage-gated sodium channels in ventricular myocytes. *Cardiovasc. Res.* 81:72–81. https://doi.org/10.1093/cvr/cvn274

Chen, X., Y. Feng, Y. Huo, and W. Tan. 2018. Effects of rogue ryanodine receptors on Ca^{2+} sparks in cardiac myocytes. *R. Soc. Open Sci.* 5:171462. https://doi.org/10.1098/rsos.171462

Cheng, H., and W.J. Lederer. 2008. Calcium sparks. *Physiol. Rev.* 88:1491–1545. https://doi.org/10.1152/physrev.00030.2007

Cheng, H., M.R. Lederer, W.J. Lederer, and M.B. Cannell. 1996. Calcium sparks and [Ca2+]i waves in cardiac myocytes. *Am. J. Physiol.* 270:C148–C159. https://doi.org/10.1152/ajpcell.1996.270.1.C148

Chopra, N., D. Laver, S.S. Davies, and B.C. Knollmann. 2009. Amitriptyline activates cardiac ryanodine channels and causes spontaneous sarcoplasmic reticulum calcium release. *Mol. Pharmacol.* 75:183–195. https://doi.org/10.1124/mol.108.051490

Curran, J., and W.E. Louch. 2015. Linking ryanodine receptor Ca^{2+} leak and Na^{+} current in heart: A day in the life of flecainide. *Acta Physiol.* 214:300–302. https://doi.org/10.1111/apha.12526

Desaphy, J.-F., A. De Luca, M.P. Didonna, A.L. George, and D. Camerino Conte. 2004. Different flecainide sensitivity of hNav1.4 channels and myotonic mutants explained by state-dependent block. *J. Physiol.* 554:321–334. https://doi.org/10.1113/jphysiol.2003.046995

Dhindwal, S., J. Lobo, V. Cabra, D.J. Santiago, A.R. Nayak, K. Dryden, and M. Samsó. 2017. A cryo-EM-based model of phosphorylation- and FKBP12.6-mediated allosterism of the cardiac ryanodine receptor. *Sci. Signal.* 10:eaai8842. https://doi.org/10.1126/scisignal.aai8842

Dulhunty, A.F., E. Wium, L. Li, A.D. Hanna, S. Mirza, S. Talukder, N.A. Ghazali, and N.A. Beard. 2012. Proteins within the intracellular calcium store determine cardiac RyR channel activity and cardiac output. *Clin. Exp. Pharmacol. Physiol.* 39:477–484. https://doi.org/10.1111/j.1440-1681.2012.05704.x

Dulhunty, A.F.. 2022. Molecular changes in the cardiac RyR2 with catecholaminergic polymorphic ventricular tachycardia (CPVT). *Frontiers in physiology.* 13:830367. https://doi.org/10.3389/fphys.2022.830367

Dulhunty, A.F., J.A. Fraser, C.L.-H. Huang, and S.C. Salvage. 2022. Gating of RYR2 channels from the arrhythmic RYR2-P2328S mouse heart and some unexpected actions of flecainide. *J. Gen. Physiol.* 154. https://doi.org/10.1085/jgp.2021ECC42

Echt, D.S., P.R. Liebson, L.B. Mitchell, R.W. Peters, D. Obiasmanno, A.H. Barker, D. Arensberg, A. Baker, L. Friedman, H.L. Greene, et al. 1991.

Mortality and morbidity in patients receiving encainide, flecainide, or placebo: The cardiac-arrhythmia suppression trial. *N. Engl. J. Med.* 324: 781–788. https://doi.org/10.1056/nejm199103213241201

Eisner, D.A., J.L. Caldwell, K. Kistamás, and A.W. Trafford. 2017. Calcium and excitation-contraction coupling in the heart. *Circ. Res.* 121:181–195. https://doi.org/10.1161/circresaha.117.310230

Fabiato, A. 1983. Calcium-induced release of calcium from the cardiac sarcoplasmic reticulum. *Am. J. Physiol.* 245:C1–C14. https://doi.org/10.1016/0022-2828(92)90114-F

Faggioni, M., D.O. Kryshtal, and B.C. Knollmann. 2012. Calsequestrin mutations and catecholaminergic polymorphic ventricular tachycardia. *Pediatr. Cardiol.* 33:959–967. https://doi.org/10.1007/s00246-012-0256-1

Fearnley, C.J., H.L. Roderick, and M.D. Bootman. 2011. Calcium signaling in cardiac myocytes. *Cold Spring Harbor Perspect. Biol.* 3:a004242. https://doi.org/10.1101/cshperspect.A004242

Fernández-Velasco, M., A. Rueda, N. Rizzi, J.P. Benitah, B. Colombi, C. Napolitano, S.G. Priori, S. Richard, and A.M. Gómez. 2009. Increased Ca^{2+} sensitivity of the ryanodine receptor mutant RyR2R4496C underlies catecholaminergic polymorphic ventricular tachycardia. *Circ. Res.* 104: 201–209. https://doi.org/10.1161/circresaha.108.177493

Fink, R.H.A., and D.G. Stephenson. 1987. Ca^{2+}-movements in muscle modulated by the state of K^+-channels in the sarcoplasmic reticulum membranes. *Pflugers Arch.* 409:374–380. https://doi.org/10.1007/BF00583791

Fink, R.H.A., and C. Veigel. 1996. Calcium uptake and release modulated by counter-ion conductances in the sarcoplasmic reticulum of skeletal muscle. *Acta Physiol. Scand.* 156:387–396. https://doi.org/10.1046/J.1365-201X.1996.212000.X

Fujii, Y., H. Itoh, S. Ohno, T. Murayama, N. Kurebayashi, H. Aoki, M. Blancard, Y. Nakagawa, S. Yamamoto, Y. Matsui, et al. 2017. A type 2 ryanodine receptor variant associated with reduced Ca^{2+} release and short-coupled torsades de pointes ventricular arrhythmia. *Heart Rhythm.* 14:98–107. https://doi.org/10.1016/j.hrthm.2016.10.015

Galimberti, E.S., and B.C. Knollmann. 2011. Efficacy and potency of class I antiarrhythmic drugs for suppression of Ca^{2+} waves in permeabilized myocytes lacking calsequestrin. *J. Mol. Cell. Cardiol.* 51:760–768. https://doi.org/10.1016/j.yjmcc.2011.07.002

Gallant, E.M., J. Hart, K. Eager, S. Curtis, and A.F. Dulhunty. 2004. Caffeine sensitivity of native RyR channels from normal and malignant hyperthermic pigs: Effects of a DHPR II-III loop peptide. *Am. J. Physiol. Cell Physiol.* 286:C821–C830. https://doi.org/10.1152/ajpcell.00311.2003

Gillespie, D., and M. Fill. 2008. Intracellular calcium release channels mediate their own countercurrent: The ryanodine receptor case study. *Biophys. J.* 95:3706–3714. https://doi.org/10.1529/biophysj.108.131987

Goddard, C.A., N.S. Ghais, Y. Zhang, A.J. Williams, W.H. Colledge, A.A. Grace, and C.L.-H. Huang. 2008. Physiological consequences of the P2328S mutation in the ryanodine receptor (RyR2) gene in genetically modified murine hearts. *Acta Physiol.* 194:123–140. https://doi.org/10.1111/j.1748-1716.2008.01865.x

Groh, S., I. Marty, M. Ottolia, G. Prestipino, A. Chapel, M. Villaz, and M. Ronjat. 1999. Functional interaction of the cytoplasmic domain of triadin with the skeletal ryanodine receptor. *J. Biol. Chem.* 274: 12278–12283. https://doi.org/10.1074/jbc.274.18.12278

Györke, S., and D. Terentyev. 2008. Modulation of ryanodine receptor by luminal calcium and accessory proteins in health and cardiac disease. *Cardiovasc. Res.* 77:245–255. https://doi.org/10.1093/cvr/cvm038

Györke, I., N. Hester, L.R. Jones, and S. Györke. 2004. The role of calsequestrin, triadin, and junctin in conferring cardiac ryanodine receptor responsiveness to luminal calcium. *Biophys. J.* 86:2121–2128. https://doi.org/10.1016/S0006-3495(04)74271-X

Henthorn, R.W., A.L. Waldo, J.L. Anderson, E.M. Gilbert, B.L. Alpert, A.K. Bhandari, R.W. Hawkinson, and E.L. Pritchett. 1991. Flecainide acetate prevents recurrence of symptomatic paroxysmal supraventricular tachycardia. The Flecainide Supraventricular Tachycardia Study Group. *Circulation.* 83:119–125. https://doi.org/10.1161/01.cir.83.1.119

Hilliard, F.A., D.S. Steele, D. Laver, Z. Yang, S.J. Le Marchand, N. Chopra, D.W. Piston, S. Huke, and B.C. Knollmann. 2010. Flecainide inhibits arrhythmogenic Ca^{2+} waves by open state block of ryanodine receptor Ca^{2+} release channels and reduction of Ca^{2+} spark mass. *J. Mol. Cell. Cardiol.* 48:293–301. https://doi.org/10.1016/j.yjmcc.2009.10.005

Hirose, S., T. Murayama, N. Tetsuo, M. Hoshiai, H. Kise, M. Yoshinaga, H. Aoki, M. Fukuyama, Y. Wuriyanghai, Y. Wada, et al. 2022. Loss-of-function mutations in cardiac ryanodine receptor channel cause various types of arrhythmias including long QT syndrome. *Europace.* 24: 497–510. https://doi.org/10.1093/europace/euab250

Hoang-Trong, M.T., A. Ullah, W.J. Lederer, and M.S. Jafri. 2021. Cardiac alternans occurs through the synergy of voltage- and calcium-dependent mechanisms. *Membranes.* 11:794. https://doi.org/10.3390/membranes11100794

Hodess, A.B., W.P. Follansbee, J.F. Spear, and E.N. Moore. 1979. Electrophysiological effects of a new antiarrhythmic agent, flecainide, on the intact canine heart. *J. Cardiovasc. Pharmacol.* 1:427–439. https://doi.org/10.1097/00005344-197907000-00005

Hwang, H.S., C. Hasdemir, D. Laver, D. Mehra, K. Turhan, M. Faggioni, H. Yin, and B.C. Knollmann. 2011. Inhibition of cardiac Ca^{2+} release channels (RyR2) determines efficacy of class I antiarrhythmic drugs in catecholaminergic polymorphic ventricular tachycardia. *Circ. Arrhythm. Electrophysiol.* 4:128–135. https://doi.org/10.1161/CIRCEP.110.959916

Hwang, H.S., M.P. Baldo, J.P. Rodriguez, M. Faggioni, and B.C. Knollmann. 2019. Efficacy of flecainide in catecholaminergic polymorphic ventricular tachycardia is mutation-independent but reduced by calcium overload. *Front. Physiol.* 10:992. https://doi.org/10.3389/FPHYS.2019.00992

Iaparov, B.I., I. Zahradnik, A.S. Moskvin, and A. Zahradníková. 2021. In silico simulations reveal that RYR distribution affects the dynamics of calcium release in cardiac myocytes. *J. Gen. Physiol.* 153:e202012685. https://doi.org/10.1085/JGP.202012685

Iyer, K.A., Y. Hu, A.R. Nayak, N. Kurebayashi, T. Murayama, and M. Samsó. 2020. Structural mechanism of two gain-of-function cardiac and skeletal RyR mutations at an equivalent site by cryo-EM. *Sci. Adv.* 6: eabb2964. https://doi.org/10.1126/sciadv.abb2964

Iyer, K.A., Y. Hu, T. Klose, T. Murayama, and M. Samsó. 2022. Cryo-EM reveals local and global structural rearrangements in RYR mutants. *J. Gen. Physiol.* 154. https://doi.org/10.1085/JGP.2021ECC44

Jiang, D., B. Xiao, L. Zhang, and S.R.W. Chen. 2002. Enhanced basal activity of a cardiac Ca^{2+} release channel (ryanodine receptor) mutant associated with ventricular tachycardia and sudden death. *Circ. Res.* 91:218–225. https://doi.org/10.1161/01.RES.0000028455.36940.5E

Jiang, D., W. Chen, R. Wang, L. Zhang, and S.R.W. Chen. 2007. Loss of luminal Ca^{2+} activation in the cardiac ryanodine receptor is associated with ventricular fibrillation and sudden death. *Proc. Natl. Acad. Sci. USA.* 104: 18309–18314. https://doi.org/10.1073/pnas.0706573104

Jorgensen, A.O., and L.J. McGuffee. 1987. Immunoelectron microscopic localization of sarcoplasmic reticulum proteins in cryofixed, freeze-dried, and low temperature-embedded tissue. *J. Histochem. Cytochem.* 35: 723–732. https://doi.org/10.1177/35.7.2953782

Kashimura, T., S.J. Briston, A.W. Trafford, C. Napolitano, S.G. Priori, D.A. Eisner, and L.A. Venetucci. 2010. In the RyR2(R4496C) mouse model of CPVT, β-adrenergic stimulation induces Ca waves by increasing SR Ca content and not by decreasing the threshold for Ca waves. *Circ. Res.* 107: 1483–1489. https://doi.org/10.1161/CIRCRESAHA.110.227744

King, J.H., C. Wickramarachchi, K. Kua, Y. Du, K. Jeevaratnam, H.R. Matthews, A.A. Grace, C.L.-H. Huang, and J.A. Fraser. 2013. Loss of Nav1.5 expression and function in murine atria containing the RyR2-P2328S gain-of-function mutation. *Cardiovasc. Res.* 99:751–759. https://doi.org/10.1093/cvr/cvt141

Knollmann, B.C. 2009. New roles of calsequestrin and triadin in cardiac muscle. *J. Physiol.* 587:3081–3087. https://doi.org/10.1113/JPHYSIOL.2009.172098

Knollmann, B.C., N. Chopra, T. Hlaing, B. Akin, T. Yang, K. Ettensohn, B.E.C. Knollmann, K.D. Horton, N.J. Weissman, I. Holinstat, et al. 2006. Casq2 deletion causes sarcoplasmic reticulum volume increase, premature Ca^{2+} release, and catecholaminergic polymorphic ventricular tachycardia. *J. Clin. Investig.* 116:2510–2520. https://doi.org/10.1172/JCI29128

Kobayashi, S., M. Yano, H. Uchinoumi, T. Suetomi, T. Susa, M. Ono, X. Xu, H. Tateishi, T. Oda, S. Okuda, et al. 2010. Dantrolene, a therapeutic agent for malignant hyperthermia, inhibits catecholaminergic polymorphic ventricular tachycardia in a RyR2(R2474S/+) knock-in mouse model. *Circ. J.* 74:2579–2584. https://doi.org/10.1253/CIRCJ.CJ-10-0680

Kornyeyev, D., A.D. Petrosky, B. Zepeda, M. Ferreiro, B. Knollmann, and A.L. Escobar. 2012. Calsequestrin 2 deletion shortens the refractoriness of Ca^{2+} release and reduces rate-dependent Ca^{2+}-alternans in intact mouse hearts. *J. Mol. Cell. Cardiol.* 52:21–31. https://doi.org/10.1016/J.YJMCC.2011.09.020

Kryshtal, D.O., D.J. Blackwell, C.L. Egly, A.N. Smith, S.M. Batiste, J.N. Johnston, D.R. Laver, and B.C. Knollmann. 2021. RYR2 channel inhibition is the principal mechanism of flecainide action in CPVT. *Circ. Res.* 128: 321–331. https://doi.org/10.1161/CIRCRESAHA.120.316819

Kuroda, Y., S. Yuasa, Y. Watanabe, S. Ito, T. Egashira, T. Seki, T. Hattori, S. Ohno, M. Kodaira, T. Suzuki, et al. 2017. Flecainide ameliorates

arrhythmogenicity through NCX flux in Andersen-Tawil syndrome-iPS cell-derived cardiomyocytes. *Biochem. Biophys. Rep.* 9:245–256. https://doi.org/10.1016/J.BBREP.2017.01.002

Langer, G.A., and A. Peskoff. 1996. Calcium concentration and movement in the diadic cleft space of the cardiac ventricular cell. *Biophys. J.* 70: 1169–1182. https://doi.org/10.1016/S0006-3495(96)79677-7

Laver, D.R., and D.F. van Helden. 2011. Three independent mechanisms contribute to tetracaine inhibition of cardiac calcium release channels. *J. Mol. Cell. Cardiol.* 51:357–369. https://doi.org/10.1016/J.YJMCC.2011.05.009

Lehnart, S.E., and W.J. Lederer. 2010. An antidote for calcium leak: Targeting molecular arrhythmia mechanisms. *J. Mol. Cell. Cardiol.* 48:279–282. https://doi.org/10.1016/J.YJMCC.2009.11.005

Lehnart, S.E., X.H.T. Wehrens, P.J. Laitinen, S.R. Reiken, S.-X. Deng, Z. Cheng, D.W. Landry, K. Kontula, H. Swan, and A.R. Marks. 2004. Sudden death in familial polymorphic ventricular tachycardia associated with calcium release channel (ryanodine receptor) leak. *Circulation.* 109:3208–3214. https://doi.org/10.1161/01.CIR.0000132472.98675.EC

Li, P., and S.R. Chen. 2001. Molecular basis of Ca(2)+ activation of the mouse cardiac Ca^{2+} release channel (ryanodine receptor). *J. Gen. Physiol.* 118: 33–44. https://doi.org/10.1085/JGP.118.1.33

Li, L., S. Mirza, S.J. Richardson, E.M. Gallant, C. Thekkedam, S.M. Pace, F. Zorzato, D. Liu, N.A. Beard, and A.F. Dulhunty. 2015. A new cytoplasmic interaction between junctin and ryanodine receptor Ca^{2+} release channels. *J. Cell Sci.* 128:951–963. https://doi.org/10.1242/JCS.160689

Liu, Q.Y., F.A. Lai, E. Rousseau, R.V. Jones, and G. Meissner. 1989. Multiple conductance states of the purified calcium release channel complex from skeletal sarcoplasmic reticulum. *Biophys. J.* 55:415–424. https://doi.org/10.1016/S0006-3495(89)82835-8

Liu, H., J. Atkins, and R.S. Kass. 2003. Common molecular determinants of flecainide and lidocaine block of heart Na^+ channels: Evidence from experiments with neutral and quaternary flecainide analogues. *J. Gen. Physiol.* 121:199–214. https://doi.org/10.1085/jgp.20028723

Liu, N., M. Denegri, Y. Ruan, J.E. Avelino-Cruz, A. Perissi, S. Negri, C. Napolitano, W.A. Coetzee, P.A. Boyden, and S.G. Priori. 2011. Short communication: Flecainide exerts an antiarrhythmic effect in a mouse model of catecholaminergic polymorphic ventricular tachycardia by increasing the threshold for triggered activity. *Circ. Res.* 109:291–295. https://doi.org/10.1161/CIRCRESAHA.111.247338

Luo, L., F. Ning, Y. Du, B. Song, D. Yang, S.C. Salvage, Y. Wang, J.A. Fraser, S. Zhang, A. Ma, and T. Wang. 2017. Calcium-dependent Nedd4-2 upregulation mediates degradation of the cardiac sodium channel Nav1.5: Implications for heart failure. *Acta Physiol.* 221:44–58. https://doi.org/10.1111/apha.12872

Martin, C.A., Y. Zhang, A.A. Grace, and C.L.-H. Huang. 2010. Increased right ventricular repolarization gradients promote arrhythmogenesis in a murine model of Brugada syndrome. *J. Cardiovasc. Electrophysiol.* 21: 1153–1159. https://doi.org/10.1111/j.1540-8167.2010.01767.x

Mehra, D., M.S. Imtiaz, D.F. Van Helden, B.C. Knollmann, and D.R. Laver. 2014. Multiple modes of ryanodine receptor 2 inhibition by flecainide. *Mol. Pharmacol.* 86:696–706. https://doi.org/10.1124/mol.114.094623

Meissner, G. 2017. The structural basis of ryanodine receptor ion channel function. *J. Gen. Physiol.* 149:1065–1089. https://doi.org/10.1085/JGP.201711878

Melgari, D., Y. Zhang, A. El Harchi, C.E. Dempsey, and J.C. Hancox. 2015. Molecular basis of hERG potassium channel blockade by the class Ic antiarrhythmic flecainide. *J. Mol. Cell. Cardiol.* 86:42–53. https://doi.org/10.1016/j.yjmcc.2015.06.021

Ning, F., L. Luo, S. Ahmad, H. Valli, K. Jeevaratnam, T. Wang, L. Guzadhur, D. Yang, J.A. Fraser, C.L.H. Huang, et al. 2016. The RyR2-P2328S mutation downregulates Nav1.5 producing arrhythmic substrate in murine ventricles. *Pflugers Arch.* 468:655–665. https://doi.org/10.1007/s00424-015-1750-0

Olubando, D., C. Hopton, J. Eden, R. Caswell, N. Lowri Thomas, S.A. Roberts, D. Morris-Rosendahl, L. Venetucci, and W.G. Newman. 2020. Classification and correlation of RYR2 missense variants in individuals with catecholaminergic polymorphic ventricular tachycardia reveals phenotypic relationships. *J. Human Gen.* 65:531–539. https://doi.org/10.1038/S10038-020-0738-6

Ormerod, J.O.M., E. Ormondroyd, Y. Li, J. Taylor, J. Wei, W. Guo, R. Wang, C.N.S. Sarton, K. McGuire, H.M.P. Dreau, et al. 2022. Provocation testing and therapeutic response in a newly described channelopathy: RyR2 calcium release deficiency syndrome. *Circ. Genom. Precis. Med.* 15: e003589. https://doi.org/10.1161/CIRCGEN.121.003589

Peng, W., H. Shen, J. Wu, W. Guo, X. Pan, R. Wang, S.R.W. Chen, and N. Yan. 2016. Structural basis for the gating mechanism of the type 2 ryanodine receptor RyR2. *Science.* 354:aah5324. https://doi.org/10.1126/SCIENCE.AAH5324

Penttinen, K., H. Swan, S. Vanninen, J. Paavola, A.M. Lahtinen, K. Kontula, and K. Aalto-Setälä. 2015. Antiarrhythmic effects of dantrolene in patients with catecholaminergic polymorphic ventricular tachycardia and replication of the responses using iPSC models. *PLoS One.* 10:e0135806. https://doi.org/10.1371/JOURNAL.PONE.0125366

Peskoff, A., and G.A. Langer. 1998. Calcium concentration and movement in the ventricular cardiac cell during an excitation-contraction cycle. *Biophys. J.* 74:153–174. https://doi.org/10.1016/S0006-3495(98)77776-8

Porta, M., A.V. Zima, A. Nani, P.L. Diaz-Sylvester, J.A. Copello, J. Ramos-Franco, L.A. Blatter, and M. Fill. 2011. Single ryanodine receptor channel basis of caffeine's action on Ca^{2+} sparks. *Biophys. J.* 100:931–938. https://doi.org/10.1016/J.BPJ.2011.01.017

Priori, S.G., C. Napolitano, P.J. Schwartz, R. Bloise, L. Crotti, and E. Ronchetti. 2000. The elusive link between LQT3 and Brugada syndrome: The role of flecainide challenge. *Circulation.* 102:945–947. https://doi.org/10.1161/01.cir.102.9.945

Priori, S.G., C. Napolitano, N. Tiso, M. Memmi, G. Vignati, R. Bloise, V. Sorrentino, and G.A. Danieli. 2001. Mutations in the cardiac ryanodine receptor gene (hRyR2) underlie catecholaminergic polymorphic ventricular tachycardia. *Circulation.* 103:196–200. https://doi.org/10.1161/01.CIR.103.2.196

Priori, S.G., A. Mazzanti, D.J. Santiago, D. Kukavica, A. Trancuccio, and J.C. Kovacic. 2021. Precision medicine in catecholaminergic polymorphic ventricular tachycardia: JACC focus seminar 5/5. *J. Am. Coll. Cardiol..* 77: 2592–2612. https://doi.org/10.1016/J.JACC.2020.12.073

Pritchett, E.L., S.D. DaTorre, M.L. Platt, S.E. McCarville, and A.J. Hougham. 1991. Flecainide acetate treatment of paroxysmal supraventricular tachycardia and paroxysmal atrial fibrillation: Dose-response studies. The flecainide supraventricular tachycardia study group. *J. Am. Coll. Cardiol.* 17:297–303. https://doi.org/10.1016/s0735-1097(10)80090-7

Ragsdale, D.S., J.C. McPhee, T. Scheuer, and W.A. Catterall. 1994. Molecular determinants of state-dependent block of Na+ channels by local anesthetics. *Science.* 265:1724–1728. https://doi.org/10.1126/science.8085162

Salvage, S.C., J.H. King, K.H. Chandrasekharan, D.I.G. Jafferji, L. Guzadhur, H.R. Matthews, C.L.H. Huang, and J.A. Fraser. 2015. Flecainide exerts paradoxical effects on sodium currents and atrial arrhythmia in murine RyR2-P2328S hearts. *Acta Physiol.* 214:361–375. https://doi.org/10.1111/apha.12505

Salvage, S.C., K.H. Chandrasekharan, K. Jeevaratnam, A.F. Dulhunty, A.J. Thompson, A.P. Jackson, and C.L.H. Huang. 2018. Multiple targets for flecainide action: Implications for cardiac arrhythmogenesis. *Br. J. Pharmacol.* 175:1260–1278. https://doi.org/10.1111/bph.13807

Salvage, S.C., E.M. Gallant, N.A. Beard, S. Ahmad, H. Valli, J.A. Fraser, C.L.-H. Huang, and A.F. Dulhunty. 2019. Ion channel gating in cardiac ryanodine receptors from the arrhythmic RyR2-P2328S mouse. *J. Cell Sci.* 132: jcs229039. https://doi.org/10.1242/jcs.229039

Salvage, S.C., E.M. Gallant, J.A. Fraser, C.L.H. Huang, and A.F. Dulhunty. 2021a. Flecainide paradoxically activates cardiac ryanodine receptor channels under low activity conditions: A potential pro-arrhythmic action. *Cells.* 10. 2101. https://doi.org/10.3390/CELLS10082101

Salvage, S.C., Z.F. Habib, H.R. Matthews, A.P. Jackson, and C.L.-H. Huang. 2021b. Ca^{2+}-dependent modulation of voltage-gated myocyte sodium channels. *Biochem. Soc. Trans.* 49:1941–1961. https://doi.org/10.1042/bst20200604

Santiago, D.J., and S.G. Priori. 2021. Cardiac ryanodine receptors: Is a severe loss-of-function not so severe after all? *Europace.* 24:494–496. https://doi.org/10.1093/europace/euab283

Santiago, D.J., J.W. Curran, D.M. Bers, W.J. Lederer, M.D. Stern, E. Ríos, and T.R. Shannon. 2010. Ca sparks do not explain all ryanodine receptor-mediated SR Ca leak in mouse ventricular myocytes. *Biophys. J.* 98: 2111–2120. https://doi.org/10.1016/J.BPJ.2010.01.042

Savio-Galimberti, E., and B.C. Knollmann. 2015. Channel activity of cardiac ryanodine receptors (RyR2) determines potency and efficacy of flecainide and R-propafenone against arrhythmogenic calcium waves in ventricular cardiomyocytes. *PLoS One.* 10:e0131179. https://doi.org/10.1371/journal.pone.0131179

Scriven, D.R.L., P. Dan, E.D. Moore, and E.D.W. Moore. 2000. Distribution of proteins implicated in excitation-contraction coupling in rat ventricular myocytes. *Biophys. J.* 79:2682–2691. https://doi.org/10.1016/S0006-3495(00)76506-4

Shimizu, W., and C. Antzelevitch. 1999. Cellular and ionic basis for T-wave alternans under long-QT conditions. *Circulation.* 99:1499–1507. https://doi.org/10.1161/01.CIR.99.11.1499

Shonts, S. 2011. Tetracaine is a potent inhibitor of SR Ca leak in ventricular cardiac myocytes. *Biophys. J.* 3495:2252. https://doi.org/10.1016/j.bpj.2010.12.2464

Sikkel, M.B., T.P. Collins, C. Rowlands, M. Shah, P. O'Gara, A.J. Williams, S.E. Harding, A.R. Lyon, and K.T. MacLeod. 2013. Flecainide reduces Ca^{2+} spark and wave frequency via inhibition of the sarcolemmal sodium current. *Cardiovasc. Res.* 98:286–296. https://doi.org/10.1093/cvr/cvt012

Sobie, E.A., S. Guatimosim, L. Gómez-Viquez, L.S. Song, H. Hartmann, M. Saleet Jafri, and W.J. Lederer. 2006. The Ca^{2+} leak paradox and rogue ryanodine receptors: SR Ca^{2+} efflux theory and practice. *Prog. Biophys. Mol. Biol.* 90:172–185. https://doi.org/10.1016/J.PBIOMOLBIO.2005.06.010

Somlyo, A.P. 1984. Cell physiology: Cellular site of calcium regulation. *Nature.* 309:516–517. https://doi.org/10.1038/309516B0

Steele, D.S., H.-S. Hwang, B.C. Knollmann, M.B. Sikkel, T.P. Collins, C. Rowlands, M. Shah, P. O'Gara, A.J. Williams, S.E. Harding, et al. 2013. Triple mode of action of flecainide in catecholaminergic polymorphic ventricular tachycardia: Reply. *Cardiovasc. Res.* 98:326–327. https://doi.org/10.1093/cvr/cvt059

Stern, M.D., L.S. Song, H. Cheng, J.S.K. Sham, H.T. Yang, K.R. Boheler, and E Ríos. 1999. Local control models of cardiac excitation-contraction coupling. A possible role for allosteric interactions between ryanodine receptors. *J. Gen. Physiol.* 113:469–489. https://doi.org/10.1085/JGP.113.3.469

Stokoe, K.S., G. Thomas, C.A. Goddard, W.H. Colledge, A.A. Grace, and C.L.-H. Huang. 2007. Effects of flecainide and quinidine on arrhythmogenic properties of Scn5a+/Delta murine hearts modelling long QT syndrome 3. *J. Physiol.* 578:69–84. https://doi.org/10.1113/jphysiol.2006.117945

Sun, B., J. Yao, M. Ni, J. Wei, X. Zhong, W. Guo, L. Zhang, R. Wang, D. Belke, Y.X. Chen, et al. 2021. Cardiac ryanodine receptor calcium release deficiency syndrome. *Sci. Transl. Med.* 13:7287. https://doi.org/10.1126/scitranslmed.aba7287

Tateishi, H., M. Yano, M. Mochizuki, T. Suetomi, M. Ono, X. Xu, H. Uchinoumi, S. Okuda, T. Oda, S. Kobayashi, et al. 2009. Defective domain–domain interactions within the ryanodine receptor as a critical cause of diastolic Ca^{2+} leak in failing hearts. *Cardiovasc. Res.* 81:536–545. https://doi.org/10.1093/CVR/CVN303

Trafford, A.W., G.C. Sibbring, M.E. Díaz, and D.A. Eisner. 2000. The effects of low concentrations of caffeine on spontaneous Ca release in isolated rat ventricular myocytes. *Cell Calcium.* 28:269–276. https://doi.org/10.1054/ceca.2000.0156

Valdes, R., S.A. Jortani, and M. Gheorghiade. 1998. Standards of laboratory practice: Cardiac drug monitoring. National academy of clinical biochemistry. *Clin. Chem.* 44:1096–1109. https://doi.org/10.1093/CLINCHEM/44.5.1096

Van Der Werf, C., P.J. Kannankeril, F. Sacher, A.D. Krahn, S. Viskin, A. Leenhardt, W. Shimizu, N. Sumitomo, F.A. Fish, Z.A. Bhuiyan, et al. 2011. Flecainide therapy reduces exercise-induced ventricular arrhythmias in patients with catecholaminergic polymorphic ventricular tachycardia. *J. Am. Coll. Cardiol.* 57:2244–2254. https://doi.org/10.1016/j.jacc.2011.01.026

Venetucci, L.A., A.W. Trafford, and D.A. Eisner. 2007. Increasing ryanodine receptor open probability alone does not produce arrhythmogenic calcium waves: Threshold sarcoplasmic reticulum calcium content is required. *Circ. Res.* 100:105–111. https://doi.org/10.1161/01.RES.0000252828.17939.00

Walker, M.A., T. Kohl, S.E. Lehnart, J.L. Greenstein, W.J. Lederer, and R.L. Winslow. 2015. On the adjacency matrix of RyR2 cluster structures. *PLoS Comput. Biol.* 11:e1004521. https://doi.org/10.1371/JOURNAL.PCBI.1004521

Walweel, K., P. Molenaar, M.S. Imtiaz, A. Denniss, C. dos Remedios, D.F. van Helden, A.F. Dulhunty, D.R. Laver, and N.A. Beard. 2017. Ryanodine receptor modification and regulation by intracellular Ca^{2+} and Mg^{2+} in healthy and failing human hearts. *J. Mol. Cell. Cardiol.* 104:53–62. https://doi.org/10.1016/j.yjmcc.2017.01.016

Watanabe, H., N. Chopra, D. Laver, H.S. Hwang, S.S. Davies, D.E. Roach, H.J. Duff, D.M. Roden, A.A.M. Wilde, and B.C. Knollmann. 2009. Flecainide prevents catecholaminergic polymorphic ventricular tachycardia in mice and humans. *Nat. Med.* 15:380–383. https://doi.org/10.1038/nm.1942

Wei, L., A.D. Hanna, N.A. Beard, and A.F. Dulhunty. 2009. Unique isoform-specific properties of calsequestrin in the heart and skeletal muscle. *Cell Calcium.* 45:474–484. https://doi.org/10.1016/j.ceca.2009.03.006

Woll, K.A., O. Haji-Ghassemi, and F. Van Petegem. 2021. Pathological conformations of disease mutant ryanodine receptors revealed by cryo-EM. *Nat. Commun.* 12:807. https://doi.org/10.1038/S41467-021-21141-3

Wolpert, C., C. Echternach, C. Veltmann, C. Antzelevitch, G.P. Thomas, S. Spehl, F. Streitner, J. Kuschyk, R. Schimpf, K.K. Haase, and M. Borggrefe. 2005. Intravenous drug challenge using flecainide and ajmaline in patients with Brugada syndrome. *Heart Rhythm.* 2:254–260. https://doi.org/10.1016/j.hrthm.2004.11.025

Woodhull, A.M. 1973. Ionic blockage of sodium channels in nerve. *J. Gen. Physiol.* 61:687–708. https://doi.org/10.1085/JGP.61.6.687

Yang, P.C., J.D. Moreno, C.Y. Miyake, S.B. Vaughn-Behrens, M.T. Jeng, E. Grandi, X.H.T. Wehrens, S.Y. Noskov, and C.E. Clancy. 2016. In silico prediction of drug therapy in catecholaminergic polymorphic ventricular tachycardia. *J. Physiol.* 594:567–593. https://doi.org/10.1113/JP271282

Yazawa, M., C. Ferrante, J. Feng, K. Mio, T. Ogura, M. Zhang, P.H. Lin, Z. Pan, S. Komazaki, K. Kato, et al. 2007. TRIC channels are essential for Ca^{2+} handling in intracellular stores. *Nature.* 448:78–82. https://doi.org/10.1038/NATURE05928

Zahradník, I., S. Györke, and A. Zahradníková. 2005. Calcium activation of ryanodine receptor channels--reconciling RyR gating models with tetrameric channel structure. *J. Gen. Physiol.* 126:515–527. https://doi.org/10.1085/JGP.200509328

Zhang, Y., J.A. Fraser, K. Jeevaratnam, X. Hao, S.S. Hothi, A.A. Grace, M. Lei, and C.L.-H. Huang. 2011. Acute atrial arrhythmogenicity and altered Ca^{2+} homeostasis in murine RyR2-P2328S hearts. *Cardiovasc. Res.* 89:794–804. https://doi.org/10.1093/cvr/cvq229

Zhang, Y., G.D.K. Matthews, M. Lei, and C.L.-H. Huang. 2013. Abnormal Ca^{2+} homeostasis, atrial arrhythmogenesis, and sinus node dysfunction in murine hearts modeling RyR2 modification. *Front. Physiol.* 4:150. https://doi.org/10.3389/fphys.2013.00150

Zhao, Y.-T., C.R. Valdivia, G.B. Gurrola, J.J. Hernández, and H.H. Valdivia. 2015a. Arrhythmogenic mechanisms in ryanodine receptor channelopathies. *Sci. China Life Sci.* 58:54–58. https://doi.org/10.1007/s11427-014-4778-z

Zhao, Y.T., C.R. Valdivia, G.B. Gurrola, P.P. Powers, B.C. Willis, R.L. Moss, J. Jalife, and H.H. Valdivia. 2015b. Arrhythmogenesis in a catecholaminergic polymorphic ventricular tachycardia mutation that depresses ryanodine receptor function. *Proc. Natl. Acad. Sci. USA.* 112:E1669–E1677. https://doi.org/10.1073/pnas.1419795112

Zhong, X., W. Guo, J. Wei, Y. Tang, Y. Liu, J.Z. Zhang, V.H. Tan, L. Zhang, R. Wang, P.P. Jones, et al. 2021. Identification of loss-of-function RyR2 mutations associated with idiopathic ventricular fibrillation and sudden death. *Biosci. Rep.* 41:BSR20210209. https://doi.org/10.1042/BSR20210209